**RESEARCH ARTICLE**

# Knockdown of Yap attenuates TAA-induced hepatic fibrosis by interaction with hedgehog signals

Ye Zhao[1] · Huiling Wang[1] · Tianhua He[1] · Bo Ma[1] · Guoguang Chen[1] · Chimeng Tzeng[2,3,4]

## Abstract

Liver fibrosis is an aberrant wound healing response to tissue injury characterized by excessive extracellular matrix deposition and loss of normal liver architecture. Hepatic stellate cells (HSCs) activation is regards to be the major process in liver fibrogenesis which is dynamic and reversible. Both Hippo signaling core factor Yap and Hedgehog (Hh) signaling promote HSCs transdifferentiation thereby regulating the repair process of liver injury. However, the molecular function of YAP and the regulation between Yap and Hh during fibrogenesis remain uncertain. In this study, the essential roles of Yap in liver fibrosis were investigated. Yap was detected to be increased in liver fibrotic tissue by the thioacetamide (TAA)-induced zebrafish embryonic and adult models. Inhibition of Yap by both embryonic morpholino interference and adult's inhibitor treatment was proved to alleviate TAA-induced liver lesions by and histology and gene expression examination. Transcriptomic analysis and gene expression detection showed that Yap and Hh signaling pathway have a cross talking upon TAA-induced liver fibrosis. In addition, TAA induction promoted the nuclear colocalization of YAP and Hh signaling factor GLI2α. This study demonstrates that Yap and Hh play synergistic protective roles in liver fibrotic response and provides new theoretical insight concerning the mechanisms of fibrosis progression.

Ye Zhao and Huiling Wang have contributed equally to this work.

✉ Ye Zhao
  zhaoyev@163.com; zhaoye@njtech.edu.cn

✉ Chimeng Tzeng
  Tzengchimeng@njtech.edu.cn

1 School of Pharmaceutical Sciences, Nanjing Tech University, Nanjing 211800, China

2 School of Pharmaceutical Sciences, Xiamen University, Xiamen 361005, China

3 Translational Medicine Research Center-Key Laboratory for Cancer T-Cell Theragnostic and Clinical Translation, School of Pharmaceutical Sciences, Xiamen University, Xiamen, Fujian, China

4 Xiamen Chang Gung Hospital Medical Research Center, Xiamen, Fujian, China

## Graphical abstract
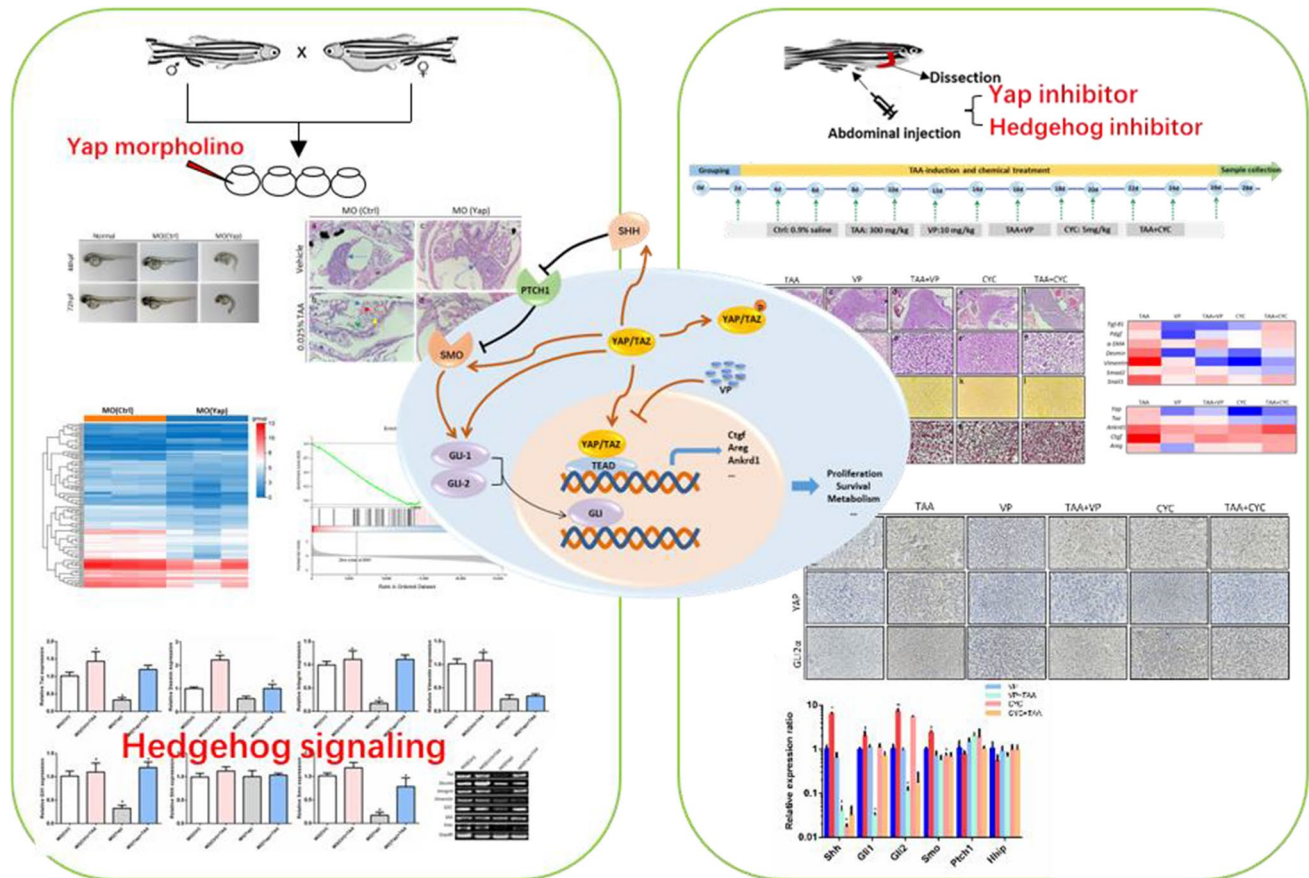


**Keywords** Yap · Hedgehog · Liver fibrosis · TAA

## Introduction

Liver fibrosis is the response to an aberrant wound healing process characterized by excessive extracellular matrix (ECM) deposition and loss of normal liver architecture (Rockey et al. 2015). Chronic liver injuries including non-alcoholic steatohepatitis (NASH), hepatitis virus infection, obesity/metabolic syndrome and biliary dysfunction are the most common causes of liver fibrosis (Ballestri et al. 2016). Progressive liver fibrosis increases the gradual formation of pathological scar tissue and ultimately, leads to end-stage liver disease, cirrhosis, hepatocellular carcinoma (HCC) and organ failure (Brunt 2010). Over the past decades, many studies believed that effective etiological treatment may reverse liver fibrosis and even early cirrhosis, not only in experimental models of liver fibrosis, but also in humans (Ellis and Mann 2012). Therefore, liver fibrosis represents a key prognostic diagnostic determinant of chronic liver diseases for clinical outcomes (Ellis and

Mann 2012). However, the current understanding of the pathogenesis of liver fibrosis is still incomplete.

Upon chronic liver damage, hepatic stellate cells (HSCs) are perpetually activated and converted into proliferative, migratory and fibrogenic myofibroblasts (Ballestri et al. 2016). Accumulation of myofibroblasts takes important roles in progressive fibrosis, defective repair and ultimately, cirrhosis (Du et al. 2018). Myofibroblastic HSCs cause up-regulation of α-smooth muscle actin (α-SMA) and Desmin, and secretion of ECM such as types I collagen (Col1a1), thereby resulting in matrix deposition and scar formation (Wells and Schwabe 2015). Myofibroblast differentiation has been recognized to be initiated by many pro-fibrogenic growth factors and cytokines. For example, transforming growth factor-β1 (Tgf-β1) and platelet-derived growth factor (Pdgf) are the key fibrogenic initiated mediators which mediates the HSCs fibroblast differentiation (Kisseleva and Brenner 2008). Profound understanding of the cellular source of activated myofibroblasts in the fibrotic liver is essential for the development of antifibrotic therapies. However, the

molecular contribution of the extracellular matrix in promotion of HSC activation remains uncertain and so far, no effective targeted therapies have been applied in the early reversible stage of liver fibrosis.

Early activation of HSC is largely driven by mechanosignaling of the extracellular microenvironment, which mediates expression of fibrillary collagens and α-SMA, leading to ECM stiffening and setting up a mechanosensitive positive feedback loop of pathological self-activation (Lodyga and Hinz 2020). Several pleiotropic cytokines such as TGF-β have provided important insight into this process (Lodyga and Hinz 2020). Recently, TGF-β has been implicated in activation of the Yes-associated protein (YAP) and Hedgehog-related fibrogenic genes expression in HSCs (Bruschi et al. 2020). YAP, as the core downstream effector of Hippo signaling pathway, mainly regulates the proper size of organs and plays a role in the progression and development of various liver diseases in cell proliferation, apoptosis, invasion and migration (Liu et al. 2019; Yu et al. 2021; Jin et al. 2021). Studies showed that the up-regulation of YAP promotes the proliferation of liver cancer cells, while the reduction of YAP effectively alleviates the entire process of HSC activation and liver fibrosis (Fang et al. 2018; Lee et al. 2019). Significantly, reduction of YAP expression has the possibility to revert the HSCs activation and impede liver fibrosis progression (Alsamman et al. 2020; Zhubanchaliyev et al. 2016). As known, YAP activity is regulated by phosphorylation, which causes YAP inactivation (Yu et al. 2019). Under physiological conditions, the Hippo pathway is activated and YAP is phosphorylated and thus retained in the cytoplasm (Halder and Johnson 2011). When in pathological conditions, the Hippo pathway is inactivated, non-phosphorylated YAP as the hyperactivation form translocates into the cell nucleus to activate downstream genes expressions, such as amphiregulin (Areg), connective tissue growth factor (Ctgf) ankyrin repeat domain 1 (Ankrd1), and affects cell biological functions (Mannaerts et al. 2015). Some studies found that in early HSC activation, Yap responses to mechanical stimulation and undergoes nuclear localization, subsequently controls waves of fibrogenic gene expression and promotes fibrogenesis (Mannaerts et al. 2015). However, in liver ischemia–reperfusion injury, study showed that YAP activation suppressed synthesis of ECM and diminished HSC activation, whereas YAP inhibition significantly delayed hepatic repair and enhanced liver fibrosis (Liu et al. 2019). The mechanistic regulation of YAP to hepatic fibrosis progression remains uncertain and even puzzled, which needs to be further investigated.

Growing evidence has identified diverse fibrogenic "driver pathways" that are the proximal mediators of the MF transition (Seki and Schwabe 2015). Among which, Yap signaling and Hedgehog (Hh), as the key morphogenic signaling pathways, take important roles in HSC activation and maintenance of myofibroblastic traits (Du et al. 2018). Hh signaling pathway, initially confirmed in Drosophila melanogaster, has been proved to be activated in liver injury and regulate liver regeneration and repair (Yan et al. 2020; Shen et al. 2017). A large amount of research evidence indicates that the Hh signaling pathway is involved in immune-mediated events that regulate fibrogenesis (Kumar et al. 2019; Wang et al. 2018).

Studies have shown that the Hh signaling pathway can activate Yap to promote the Hippo pathway, thereby regulating the repair process of liver injury (Yan et al. 2020; Swiderska-Syn et al. 2016; Oh et al. 2018). Actually, both Hh and Yap activity are negligible and confined to small subpopulations of stromal cells in healthy adult liver in which most HSCs are quiescent (Du et al. 2018). Upon damage stimulation, Hh pathway and Yap activities are dramatically activated in both HSC and hepatocytes (Swiderska-Syn et al. 2016). Moreover, the HSC transdifferenciation and sustain of the status require activation of both Hh pathway and Yap simultaneously (Yu et al. 2019; Choi et al. 2009). Disruption of Hh or prevention of Yap is sufficient to prevent HSCs activation despite ongoing exposure to fibrogenic induction (Swiderska-Syn et al. 2016). Furthermore, Hh signaling drives HSCs transdifferentiation by activating Yap, whereas inhibition of Hh signaling blocked the Yap activation (Du et al. 2018; Swiderska-Syn et al. 2016). Knockdown of Yap inhibited both Yap- and Hh-regulated genes associated with HSCs activation in cultured HSCs (Du et al. 2018; Swiderska-Syn et al. 2016). Inordinate activation of either the Hh signaling or Yap can lead to defective repair that promotes the process of liver fibrosis, cirrhosis and even cancer (Swiderska-Syn et al. 2016; Nguyen et al. 2015). The mechanisms that coordinate the activities of Hh signaling and Yap activity during liver fibrosis remains to be further clarified. Bearing this in mind, our research aims to investigate the role of Yap and interactions between Yap and Hh signaling pathway during the process of fibrotic liver injury.

# Materials and methods

## Zebrafish husbandry

Zebrafish husbandry was according to the compliance with Institutional Animal Care and Use Committee (IACUC) guidelines of Nanjing Tech University for laboratory animal use. Adult wild-type zebrafish Tübingen (TU) line were provided by Model Animal Research Center of Nanjing University (Nanjing, China). Fish were maintained in closed flow-through system with ventilated circulating water under the standardized conditions of temperature ($28 \pm 0.5$ °C), pH ($7.0 \pm 1.0$), and in a 14-h light/10-h dark rotation as reported (Zhao et al. 2020). Fishes were fed twice to three times daily

with live brine. Fish spawning was implemented artificially by the onset of light stimulation, with the male–female ratio of 1:2 for mating. In the process of breeding, abnormally fertilized embryos were removed in time. After 3 days development, normally fertilized embryos were fed paramecium culture and AP100 (Shanghai FishBio Co., Ltd, China) daily. Adult zebrafish were randomly used without sex bias. Three-months old fish were used and at least three individual samples were collected for all assays.

## Morpholinos and microinjection

Morpholino (MO) antisense oligonucleotides of Yap as MO (Yap) (5′-CTCTTCTTTCTATCCAACAGAAACC3′), and control as MO (Ctrl) (5′-CCTCTTACCTCAGTTACAATT TATA-3′) were obtained from Gene Tools, LLC (USA) as described (Hu et al. 2013). One to two-cell stage wildtype zebrafish embryos were microinjected with MOs (5 ng/embryo) using a pressure microinjector (IM-300 Narishige, Japan).

## Zebrafish intraperitoneal injection

Adult zebrafish fish underwent fasting for 24 h were placed in the experimental tank with fish facility water, and ice chips were slowly added into the container to bring the water temperature down to 12 °C. The surgical plane of anesthesia was approached when fish stop swimming and gasping, and the operculum movements were slowdown (Kinkel et al. 2010). After anesthetized, zebrafish were gently moved to the sponge trough and injection was implemented into the abdominal cavity, posterior to the pelvic girdle. After injection, fish were immediately transferred back to warm water with the temperature about 28.5 °C for recovery. 35G beveled steel needle and a 10 µl NanoFil microsyringe (Shanghai Gaoge Co., Ltd, China) were applied in experiments.

## Chemical allocation and administration

In zebrafish embryo experiments, MO (Yap) (5 ng/nl) and MO (Ctrl) (5 ng/nl) were injected at the one to two-cell stage of embryos with 1 nl per embryo (Hu et al. 2013). After 72 h post fertilization (hpf), half of the two groups were cultured with 0.025% thioacetamide (TAA, Shanghai Saen Chemical Technology Co. Ltd. China) for 3 days (Amali et al. 2006a; Rekha et al. 2008), and the other half were kept in culture water. In the adult fish experiments, fish were randomly divided into six groups with 30 fish in each group. Control group (shown as Ctrl): zebrafish were injected with equal volume of saline; TAA group (shown as TAA): each fish was intraperitoneally injected with TAA (300 mg/kg body weight) which induces fibrosis in zebrafish liver (Hammes et al. 2012; Chuang et al. 2016); Verteporfin

(VP, Sigma, USA) group (shown as VP): VP was diluted to different concentrations using dimethyl sulfoxide (DMSO). Zebrafish were injected with VP (10 mg/kg bodyweight) intraperitoneally; VP + TAA group (shown as VP + TAA): each zebrafish was intraperitoneally injected with TAA (300 mg/kg bodyweight) and VP (10 mg/kg body weight) (Lin et al. 2020); Cyclopamine (CYC, Aladdin, Shanghai, China) group (shown as CYC: zebrafish was injected with CYC (5 mg/kg bodyweight) intraperitoneally (Reimer et al. 2009); CYC + TAA group (shown as CYC + TAA): each zebrafish was injected CYC (5 mg/kg bodyweight) and TAA (300 mg/kg bodyweight) (Zhang et al. 2017; Li et al. 2015) intraperitoneally. The chemicals were administered by intraperitoneal injections three times per week for 4 weeks (Chuang et al. 2016).

## Liver function test

Alanine aminotransferase (ALT) activity assay kit (MAK052, Sigma-Aldrich) was applied to evaluate the liver function of zebrafish. After exposure, adult zebrafish blood was collected using a heparinized glass capillary needle from the region of dorsal aorta. Ten blood samples were pooled as one replicate (about 10 µl). Plasma was obtained as clear supernatant by centrifugation at 1000g for 10 min using a refrigerated centrifuge and stored at −80 °C. Plasma ALT was measured following the manufacturer's protocol. There were three replicates for each group.

## Reverse transcription-polymerase chain reaction (RT-PCR) and quantitative RT-PCR

Total RNA was isolated and purified using TRIzol reagent (Invitrogen, Carlsbad, CA, USA) from random pooled ten zebrafish larvae or ten livers dissected from adult fish and purified using the RNease Mini Kit (Qiagen, USA), according to the instructions. Total RNA concentrations were quantified with a nucleic acid and protein spectrophotometer (Nano-300, Aosheng Instrument Co., Ltd., Hangzhou, China). RNA integrity was determined by electrophoretic analysis of 28S and 18S rRNA subunits with clearly ribosomal RNA bands brightness ratio of approximately 2:1. Complimentary DNA was synthesized using the SuperScript II cDNA Synthesis Kit (Invitrogen, USA) from 5 µg of total RNA. DNA was quantified and OD260/280 was calculated for estimation of the purity by spectrophotometric analysis. The ratio of OD260/OD280 from 1.8 to 2.0 were chosen for the next steps. Power SYBR Green Master Mix (Applied Biosystems, Thermo Fisher Scientific, USA) was used for real-time quantitative reverse transcription polymerase chain reaction (qRT-PCR) analysis. Primers were designed using PRIMER 5 software and purchased from GenScript, China and melting curves were performed to verify primer

specificity (Table 1). The glyceraldehyde-3-phosphate dehydrogenase (Gapdh) mRNA was used as a control for calibration of gene expression levels between different samples (Gao et al. 2015). All reactions were triplicated. Log2 fold changes were calculated between samples and control by the $-\Delta\Delta CT$ method. The log2 fold changes in target gene relative to reference gene Gapdh were calculated following this formula: log2 fold changes $= -\Delta\Delta CT = -[($Ct$_{\text{Target}}$ − Ct$_{\text{Gapdh}}$) test − (Ct$_{\text{Target}}$ − Ct$_{\text{Gapdh}}$) control]. The Ct (cycle threshold) values were defined as the number of PCR amplification cycles at which the fluorencent signals were detected (Livak and Schmittgen 2001). Two-tailed heteroscedastic t test was performed using normalized Ct values (Ct$_{\text{Target}}$ − Ct$_{\text{Gapdh}}$) and $p < 0.05$ was considered to be significant. Conventional PCR was applied as for primer specificity verification and semi-quantitative validation.

## Western-blot analysis

Protein samples of zebrafish embryos were lysed in Radio Immunoprecipitation Assay (RIPA) buffer and separated in the 12% SDS–polyacrylamide gel electrophoresis (PAGE). The blots were then transferred to a nitrocellulose membrane (Bio-Rad, USA). The membranes were incubated with YAP1 (Proteintech, USA) at 1:1000 or GAPDH (Proteintech, USA) at 1:5000 dilutions in TBS containing 1% skim milk; the blots were then incubated with secondary antibodies, HRP-conjugated goat anti-mouse IgGs (Zhongshanjinqiao Co. China) at 1:2000. The experiments were repeated three times with different samples.

## RNA transcriptomic analysis

Total RNA was isolated and RNA quality was checked by Agilent 2100 Bioanalyzer (Agilent Technologies, Palo Alto, CA, USA). RNA sequencing was carried on after library construction by next-generation Illumina HiSeq 2000 by Beijing Genome Institute (BGI, Shenzhen, China). Raw reads obtained were filtered to remove the adaptor sequences and low complexity sequences and empty reads. The sequence reads were mapped to the zebrafish reference sequence database (*Danio rerio*, UCSC version danRer7, 2010) using TopHat2.0 (http://ccb.jhu.edu/software/tophat/index.shtml) (Lam et al. 2006). Differentially expressed genes (DEGs) between samples was determined by $p < 0.05$ and absolute fold changes (FCs) > 2 using DESeq2 as described (Huo et al. 2019a).

Then DEGs were analyzed by the Database for Annotation, Visualization and Integration Discovery (DAVID) Functional Annotation (https://david.ncifcrf.gov/home.jsp) to obtain Gene ontology (GO) annotations. Kyoto Encyclopedia of Genes and Genomes (KEGG) pathway analyses were performed using KEGG pathway database (http://www.kegg.jp/kegg/pathway.html). Gene set enrichment analysis (GSEA) was performed to analyze the molecular pathway enrichment of candidate gene by GSEA 3.0 according to published methods (Huo et al.

**Table 1** Primers sequences

| Gene | Gene ID | Forward sequence | Reverse sequence |
| --- | --- | --- | --- |
| Gapdh | 317743 | CCAACTGCCTGGCTCCTT | CCCATCAACGGTCTTCTGTG |
| Ankrd1 | 564159 | GCAGACCCAAATGCATGTGATA | ATGAAGAGCAGTGCTGCGAA |
| Ctgf | 321449 | AATGGTGTACCGCAGTGGAG | GGGACCGTATGTCTCCTCCT |
| Areg | 101884611 | AAGGAGACGAGCAGAACCAC | AGCGCTCACCATCATAACCT |
| Yap | 561411 | GAACCCGAAAAACACCATCGTCCCC | GACTGGCGGAGGTGCTGAGGTGGGG |
| Taz | 321965 | GGTGGGCTCATACAGTTACCTTTGG | GAGGCAGCAGGTGTCCATCTCATCT |
| Tgf-β1 | 21803 | GTCCGAGATGAAGCGCAGTA | GGAGACAAAGCGAGTTCCCA |
| Pdgf | 386856 | ACAAGGCCACCATAAGGAGC | GATCCACCTGACTTCGTGGG |
| Smad2 | 30639 | CATGTCATCTACTGCCGCCT | TCTGTGTGTCTTGGCACGAG |
| Snail1 | 30273 | GCTTCCAGCAGTCAGCAATG | GTCTGACGTCCGTCCTTCAT |
| Desmin | 108267036 | GAGGAGGCAAATGAGTGAGATGGAG | TTGGAGTGGACTTCAGATGAGCGTT |
| Vimentin | 140599 | TTCGCCAGTTACATAGACAAAGTGC | AGACGAGCCAGAGAGGCGTTATCAA |
| α-SMA | 322509 | CTCTGTTGACAGAAGCCCCA | GGCCAAGTCCAAACGCATAA |
| Shh | 30269 | CGGTTGCTGCGAAATCTGGGGGCTG | GCGTCGTGGAGTCTCGGTCTGTGAA |
| Ptch1 | 30189 | GGCAGCTAATCTGGAGACGG | AGCGCCTCTACGGTCAAAAT |
| Hhip | 326102 | GAGGAGATGGATGGTCTGAGTGATT | GGATTGTTTCTGGGTATGGAGTAGG |
| Smo | 30225 | GGTTGAGAAATGCTCCTCGCTGTTG | CCCCTCTCCCGCTCCACAATACTGC |
| Gli1 | 352930 | ACTGGAATGTCCTGCCCTCCGAACG | GAGCGTCTGCTGGACAGGTATGGCG |
| Gli2α | 30154 | ACAAGGCTTTTTCCAACGCTTCAGA | ACGTTTTGTGCAACCTGGGATCTTA |

2019b). The terms of gene expression values of the control and Yap knockdown groups were deemed as statistically significant when the statistical significance of enrichment score was estimated by $p < 0.05$. Hippo signaling gene sets were obtained from the Molecular Signatures Database (MSigDB) v6.1.

## Histopathological analysis

Zebrafish were euthanized after anesthesia with 0.1 mg/ml Tricaine (Sigma-Aldrich) and fixed with 4% paraformaldehyde (PFA) in phosphate-buffered saline (Sigma-Aldrich) and paraffin-embedded. The fish liver was cut into five-micrometer thickness sections by microtome. Hematoxylin and eosin (H&E) staining (H-3404, Vector labs, USA), Sirius Red Staining (24901, Polyscience, USA), Nile red (7385-67-3, Macklin, China) staining and Masson's trichrome (GP1032, Servicebio, China) staining were performed following standard protocols. Histopathological changes were determined based on the previous study (Henderson et al. 2018); Nile red labeled the neutral lipid properties with red fluorescence was observed under an emission maximum of about 638 nm; Liver fibrosis histological sections stained with Sirius red and Masson's trichrome were evaluated with digital images produced using the Image J software (developed by National Institutes of Health) as described (Zhao et al. 2016). At least three sections from each treatment group were microphotographed by inverted microscope (Nikon ECLIPSE Ts2, Japan).

## Immunohistochemistry and immunofluorescence assay

Zebrafish were fixed in 4% PFA, embedded in paraffin and sectioned at five-micrometer thickness. For immunohistochemistry staining, the tissues were blocked with 3% normal non immune serum, and antigens were detected using primary antibodies Gli2a (GTX128280, GeneTex, USA), α-SMA (E20-53365, Enogene, China) and YAP1 (13584-1-AP, Proteintech, USA) in conjunction with an HRP/DAB (ABC) detection kit (ab64264, Abcam, USA) following manufacturer's protocols. For immunofluorescence detection, FITC-conjugated secondary goat anti-mouse antibodies (Vector Laboratories, USA) and the Cy3-conjugated anti-rabbit secondary antibody (1: 250; Dianova, Hamburg, Germany) were applied and the cell nuclei were stained with DAPI (4′, 6-diamidino-2-phenylindole, 300 ng/ml, Sigma). Sections were observed under aforementioned fluorescent microscope at 543 nm for CY3, 488 nm for FITC and 360 nm for DAPI, respectively. Quantifications of immunofluorescence assays were performed using Image J.

## Statistical analysis

All experiments were repeated at least three times independently. Statistical analysis was performed using GraphPad Prism 6 (GraphPad Software, San Diego, California, USA). The difference of two groups was confirmed by Student's t-test and the difference of multiple groups was defined through a one-way analysis of variance (ANOVA) with Tukey's honestly significant difference test (Tukey's HSD) at a significance level of 0.05. All data are presented as mean values ± standard deviation (SD).

## Results

### Knockdown of Yap gene alleviates TAA-induced embryonic liver lesions

Previous studies have demonstrated that Yap plays pivotal roles in various liver diseases such as hepatocellular carcinoma, non-alcoholic fatty liver and liver regeneration after partial hepatectomy, etc. (Johnson 2019). Although widely expressed in liver and other digestive organs in zebrafish embryos, Yap knockout did not display visible defects during embryogenesis (Yi et al. 2018). The roles of Yap in embryonic liver development are unclear so far. Here, to investigate the function of Yap in embryonic liver development in zebrafish, Yap morpholino oligos (MO), MO (Yap) and control morpholino oligos, MO (Ctrl) were individually microinjected into embryos at the one- to two-cell stage, in which MO (Yap) can complementarily bind to the initial sequence of Yap mRNA and inhibit the translation of YAP protein. The results from both mRNA and protein detection showed the MO (Yap) microinjection blocked Yap expression (Fig. 1A, B), consistent with the previous study (Jiang et al. 2009). Additionally, the loss of Yap expression exhibits the embryonic deformities, such as pericardial edema, smaller and incomplete eyes, notochord deformities, shortened body trunk, tail and yolk extension, etc. (Fig. 1C). At 72 h post fertilization (hpf), the malformation rate of Yap knockdown group was 18.76%. No mortality has been detected at 72 hpf (data not shown).

Liver function was further investigated by Nile red and H&E staining. TAA with the concentration of 0.025% from 72 hpf to 7 days post fertilization (dpf) was used to induce liver fibrosis and steatohepatitis in zebrafish embryos (Amali et al. 2006; Helm et al. 2018). In Fig. 1D and E, the Nile red staining results showed that the liver size was remarkably increased after TAA treatment. The liver size was decreased in knockdown of Yap in TAA group compared to the non-knockdown control. Moreover, the red fluorescence intensity in the liver was significantly enhanced in TAA treatment group as compared to control (Fig. 1D, F). Yap
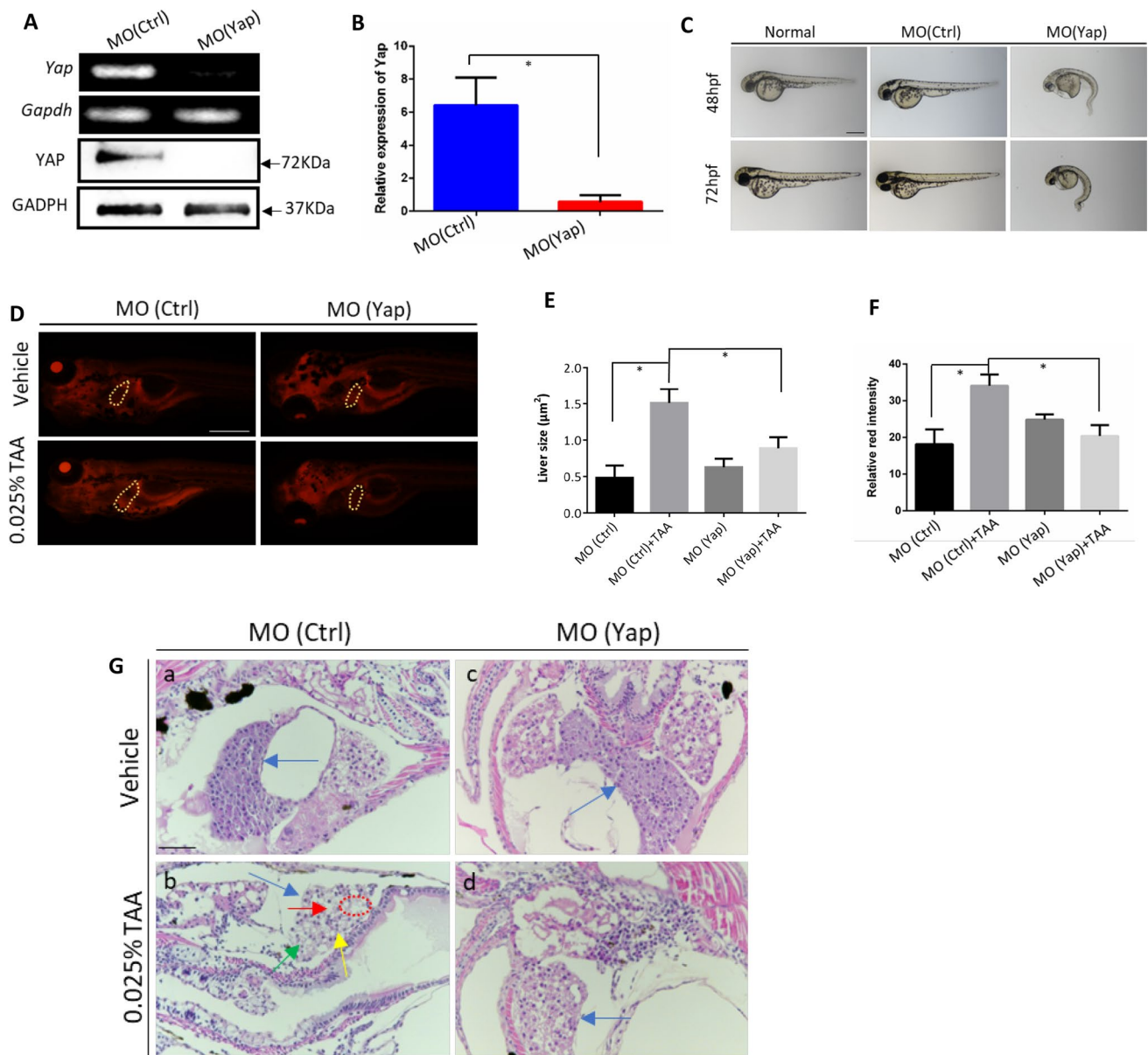
**Fig. 1** Analysis of morphant phenotype and TAA-induced embryonic liver lesions caused by Yap knockdown. **A** Validation of Yap knockdown by RT-PCR and Western blot analysis. Total RNA and proteins were extracted from 24 hpf zebrafish embryos in MO (Yap) and MO (Ctrl) (n = 10). **B** Validation of Yap knockdown by qPCR. **C** Morphant observation of 48 and 72 hpf embryos injected with MO (Yap) (5 ng/embryo), MO (Ctrl) (5 ng/embryo), and non-injected normal embryos. **D** Nile red-stained sections of embryos with the treatment of 0.025% TAA from 72 hpf to 7 dpf. **E** Qualifications of liver size in each group, n = 5. **F** Qualifications of Nile red staining by relative red intensity by ImageJ (n = 5). Data are shown as means ± SEM. *$p < 0.05$. **G** Histological evaluations of zebrafish liver by hematoxylin and eosin (H&E) with the treatment of 0.025% TAA from 72 hpf to 7 dpf

knockdown did not cause statistical changes by fluorescence quantification. Interestingly, compared with TAA-induced liver fibrosis group, Yap knockdown after TAA treatment caused a significantly decrease of red fluorescence intensity in the liver, which reveals that inhibition of Yap may have a potential effect in alleviation of TAA-induced liver defect in hepatomegaly and neutral lipid deposition. In H&E staining (Fig. 1G), livers were indicated by the blue arrows.

The vehicle control showed that normal liver tissue presents normal tight junctions, a clear polygonal shape, with complete and prominent cytoplasm and nucleus (Fig. 1Ga). However, in the TAA-treatment group with MO (Ctrl) injection, the zebrafish embryonic liver appeared dissociated and irregular cell shape, loosen cell-to-cell contact, with various levels of tiny and large vacuoles inside. To be more, macrovesicular steatosis was easy to be identified (as indicated

by the red arrow). The contours of liver parenchymal cells are destroyed, and some part showed nuclear shrinkage (as indicated by the yellow arrow), nuclear lysis (as indicated by the green arrow), and focal necrosis (as indicated by the red circle) characteristics. (Fig. 1Gb). In the MO (Yap) injection group, the liver showed no obvious difference with vehicle group, with normal cell structure and tight cell contacts, and the liver was filled with well-delineated polygonal cells with well-preserved cytoplasm and clear nucleus (Fig. 1Gc). Compared with the MO (Ctrl) group treated with TAA, the liver of the MO (Yap) group treated with TAA showed a rescue effect on TAA induced liver damage (Fig. 1Gd). The loosely arranged liver parenchymal cells was ameliorated, and most of large vacuoles inside cells disappeared. The liver parenchymal cells with well-preserved cytoplasm and clear nucleus increased and no obvious degeneration (edema) and steatosis or necrosis can be observed. Therefore, embryonic gene knockdown of Yap alleviates TAA-induced embryonic liver lesions.

## Transcriptome profiling of Yap knockdown reveals its essential functions in embryonic liver development

To identify potential molecular function of Yap during embryonic liver development, RNAs isolated from these MO (Yap) and MO (Ctrl) with three biological replicates were sequenced and transcript expression was comparatively analyzed mapping to the zebrafish RefSeq database. A total of 1596 differentially expressed genes (DEGs) were identified differential expression in MO (Yap) compared with MO (Ctrl), including 1244 down- and 352 up-regulated DEGs ($|\log2FC| \geq 1$, Q value $\leq 0.001$). By hierarchical clustering based on DEG expression patterns, as shown in Fig. 2A, the Yap knockdown samples MO (Yap) were clustered as similar relationship and well separated from all control samples MO (Ctrl), suggesting that there were substantial changes caused by Yap knockdown. Volcano maps of expression distribution of these DEGs are displayed according to their fold change, of which the top 10 down-regulated DEGs were labeled (Fig. 2B).

To predict the molecular function of Yap, DEGs were subjected to KEGG pathway analysis to identify the associated pathways and molecular interactions. Items with corrected *p* values less than 0.05 were considered to be significant or enriched. The KEGG gene set biological process database (c2. KEGG. v4.0) from the Molecular Signatures Database was used for enrichment analysis. As shown in green dashed circle of Fig. 2C, the top five enriched KEGG pathways associated with the downregulated mRNA transcripts are focal adhesion, TNF signaling pathway, extracellular matrix receptor interaction, regulation of actin cytoskeleton and IL-17 signaling pathway, all of which are

highly related with HSCs activation, liver fibrosis progression and hepatocellular carcinoma (Ma et al. 2020; Villesen et al. 2020). For the enriched KEGG pathway of upregulated DEGs, most of which are related with cell metabolism, such as fat digestion, glycolysis, protein digestion and absorption, etc. The results indicated that Yap knockdown downregulated the signaling pathways concentrated on liver fibrotic injuries.

To gain more detailed functional insights into the molecular function related with Yap knockdown, GO analysis was conducted to perform an unbiased annotation of the functions of these downregulated 1244 DEGs including three functional clusters: biological process (BP), molecular function (MF) and cellular component (CC). Among the downregulated DEGs in the Yap knockdown group, the cluster of biological processes were found to be mainly relative to integrin-mediated signaling pathway, cell adhesion, cell matrix adhesion, cell adhesion mediated by integrin, which are closely associate with HSC activation and liver fibrosis (green dashed circle in Fig. 2D). In addition, platelet aggregation, neutrophil migration and inflammation response related processes are also downregulated in MO (Yap) compared with controls. Meanwhile, GO analysis showed that in the molecular function, these downregulated DEGs were mainly related to collagen binding in cell–matrix adhesion, integrin binding, tumor necrosis factor activated receptor activity (Fig. 2Db). With regard to molecular functions, these genes were mainly enriched in integrin complex, exocellular region, extracellular matrix and focal adhesion (Fig. 2Dc). Collectively, the results of GO annotation indicated the similar results as KEGG analysis, both of which implied that Yap knockdown may take potential roles in liver fibrotic injury.

## Yap knockdown is correlated with Hh signaling based on GSEA analysis

GSEA has been designed to investigate the coordinated differences in gene expression from predefined sets of functionally related genes to identify pathways that are significantly changed (Subramanian et al. 2005). To further investigate the possible pathways coordinately down-regulated by knockdown of Yap, the transcriptomic data were compared by GSEA. In the analysis, GSEA firstly generated an ordered list of all genes according to their correlation with Yap knockdown and then a predefined gene set (signature of gene expression upon perturbation of certain cancer-related gene) receives an enrichment score (ES), which is a measure of statistical evidence rejecting the null hypothesis that its members are randomly distributed in the ordered list. Among all the 195 predefined KEGG pathway gene sets, the Hippo signaling pathway (Enrichment plot: 04390) were identified as having a significant association with Yap
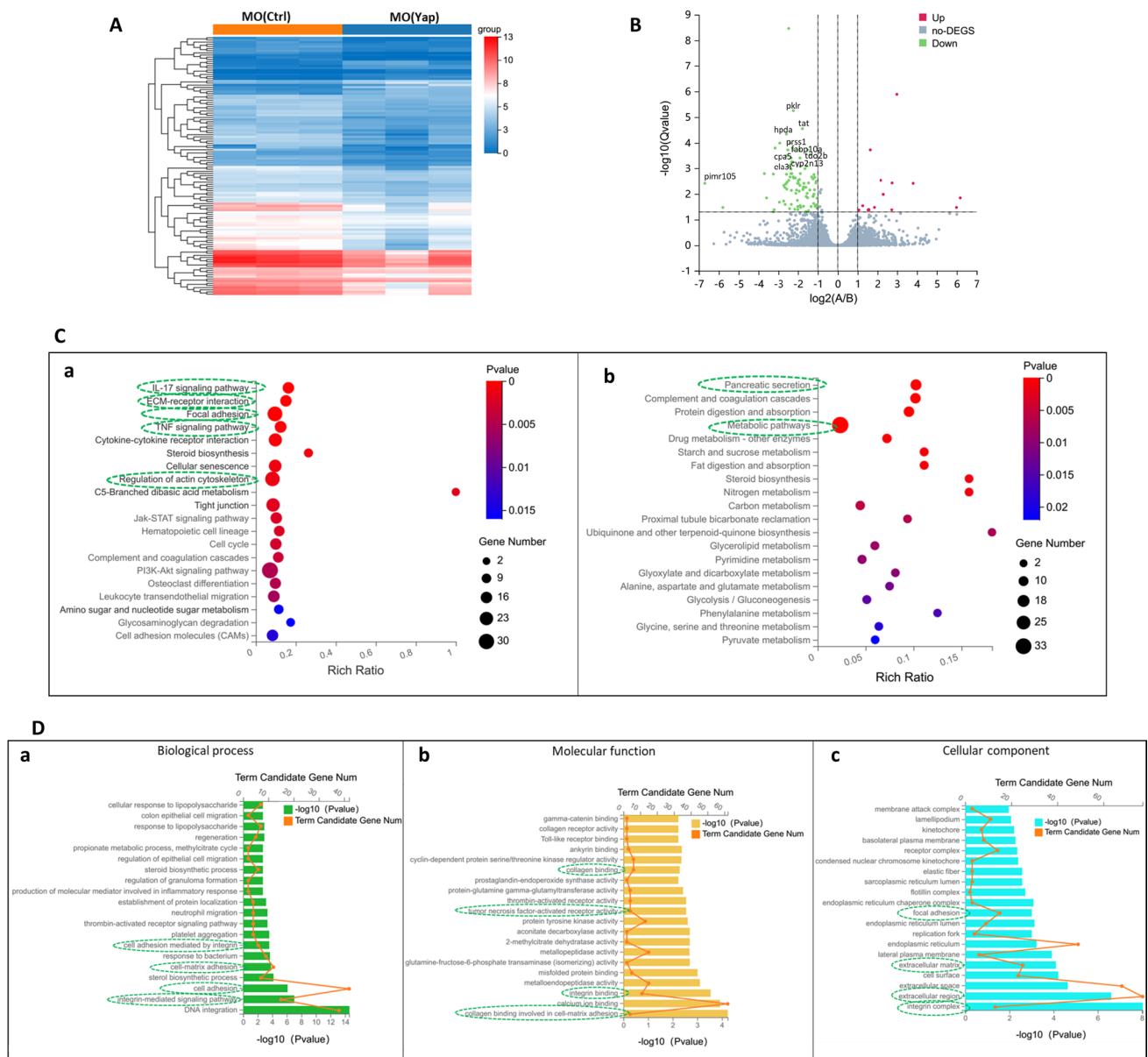
**Fig. 2** Global transcriptomic analysis and knockdown of Yap mediated signatures in zebrafish embryos. **A** Hierarchical clustering of RNA-Seq data shows global gene expression changes between the MO (Ctrl) and MO (Yap). High and low expression levels of genes are represented by red and blue. Gene expression (TPM) is log2-transformed and median-centered across genes. **B** Groups at mRNA level are shown in volcano plots of log2 (fold change) versus −log10 (*p* value). Red dots indicate up-regulated DEGs, the green dots indicate down-regulated DEGs, and blue dots represent non-DEGs. The top ten down-regulated transcripts, ranked by their distance to the base point are marked. **C** KEGG enrichment analysis of DEGs. Top 20 KEGG pathways among the down-regulated (**a**) or (**b**) up-regulated DEGs were presented in bar charts. **D** GO analysis of downregulated DEGs mediated by Yap knockdown. Top 20 GO in the three categories: biological process (**a**), molecular function (**b**) and cellular component (**c**) of significantly down-regulated DEGs were presented in bar charts

expression in the liver function (Fig. 3A). In addition, we also explored the canonical pathways that are enriched by analysis of the predefined gene set using KEGG. Hedgehog (Hh) signal, Wnt signaling pathway, TGF-β signaling pathway, etc. were identified among the top enriched canonical pathways in crosstalk with hippo pathway upon Yap knockdown (Fig. 3B). Interestingly, these results suggested that Hh

signaling pathway has a crosstalk with Yap downregulation during embryogenesis.

Furthermore, to explore the dynamic range of gene expression of Hh and its correlation with Yap knockdown under normal development and embryonic liver injury, qPCR was performed. The effector of the Hippo pathway TAZ (transcriptional coactivator with PDZ-binding motif),
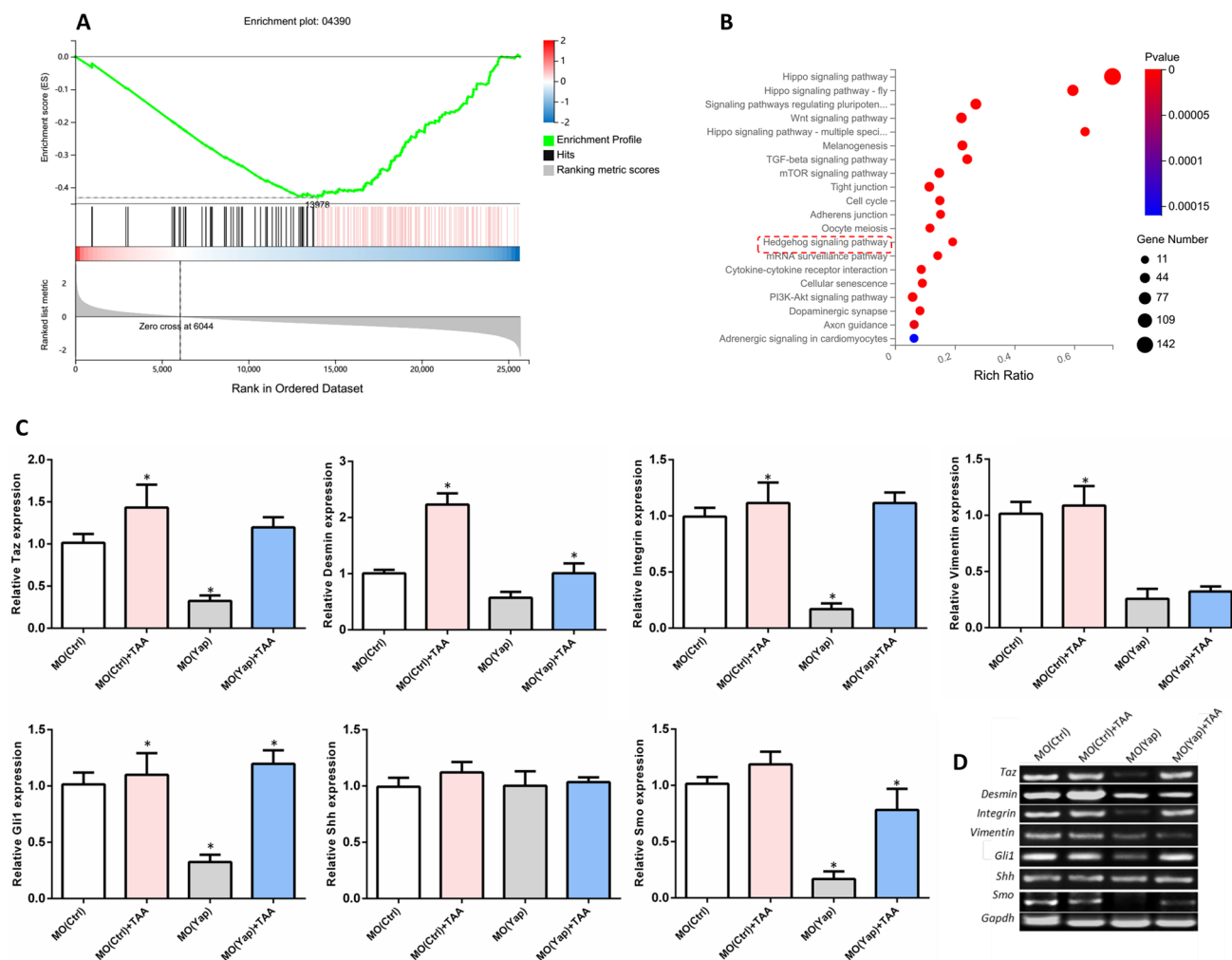
**Fig. 3** Gene set enrichment analysis (GSEA) was performed using the Molecular Signatures Database. **A** Downregulated genes compared from MO (Yap) to MO (Ctrl) as signatures were enrichment by GSEA. **B** An enrichment of predefined genes within Hippo pathway by GSEA were analyzed by KEGG. Top 20 KEGG pathways among were showed. **C** Quantitative PCR for mRNA expression. Values are expressed as means ± SD. *$p < 0.05$ for treatment groups versus control. **D** Conventional PCR was as the validation

liver fibrosis-related expression factors Desmin, Vimentin and Integrin, and Hh signaling molecules Gli1 (GLI family zinc finger 1), signaling molecules sonic hedgehog (Shh) and G protein-coupled receptor Smoothened (Smo) were selected to detect the expression levels. Results in Fig. 3C showed that TAA induction significantly increased the expression of Taz, Desmin and Integrin, and Hh signaling factors Gli1. And the knockdown of Yap significantly inhibited the expression Taz, integrin and Hh signaling factors Gli1 and Smo, which implied an interaction between and Hh signaling. MO (Yap) has a reversal effect on the increase of liver fibrosis-related factors Desmin, Integrin induced by TAA, as well as a reversal effect on the increase of Hh signal factor Gli1 and Smo after TAA induction. However, no significant changes were detected in Hh signal molecules Shh. The results were validated by conversional PCR (Fig. 3D).

## Yap knockdown has an inhibitory effect on TAA-induced liver changes in adult zebrafish

The transcriptomic analysis revealed that Yap knockdown is associated with liver fibrotic injury and has a crosstalk with Hh signaling. To further validate the role of Yap knockdown and the correlation with Hh in liver injury, we induced liver fibrosis in adult zebrafish using TAA, and examined the effects of Yap inhibitor VP and Hh inhibitor CYC by histology and gene expression. The experimental flow chart for chemical treatments and time points of sampling is shown in Fig. 4A. Randomly selected adult zebrafish (3 months old) were abdominal injected with control (0.9% saline, 5 μl), TAA (300 mg/kg body weight), VP (10 mg/kg body weight), CYC (5 mg/kg body weight), or the mixture of TAA and VP, TAA and CYC with the same dosage, respectively. High ALT level is considered to be an important sign of

liver damage. Zebrafish plasma ALT levels at 28 days after treatment were tested in triplicate (n = 10 per replicate). Results indicated a remarkable increasing of ALT level in TAA treated groups compared to the untreated control group (Fig. 4B). Notably, VP was able to reverse the ALT elevation significantly, indicating that VP relieved liver injury caused by TAA. Moreover, liver tissue of zebrafish at 28 days after treatment were collected with five replicates. In Fig. 4Ca–f, histological examinations for samples stained with H&E under the magnification of 40× showed that VP- and CYC-treated livers, and TAA + VP livers appeared to be homogeneous, as well as the control fish. TAA-treated and TAA + CYC showed apparent degree of histopathological heterogeneity of liver parenchyma. At a higher magnification of 400×, the livers parenchyma from TAA-treated and the TAA + CYC groups appeared to be loosen in cell contact and the polygonal cell structure collapsed, accompanied by nuclear dissolution and the formation of large vacuoles and scar-like structures, which revealed steatosis and fibrosis in these groups (Fig. 4Ca, c, d and e). However, the groups of VP-, TAA + VP and CYC-treated livers exhibited well-delineated polygonal cells with tight contacts and complete nucleus, as almost the same as normal control (Fig. 4Ca′–f′). Quantitative analysis of H&E was performed based on the measurement of necrotic area in livers (Fig. 4Cs). Results suggested that VP had an inhibitory effect on TAA-induced liver lesions.

To analyze the collagen deposition in the adult liver, Sirius-red staining was performed. Results showed that TAA-induced liver exhibited characteristic fibrous connective tissue (Fig. 4Ch). These results revealed the subtle structures of collagen deposition between the hepatocytes and a possible onset of fibrogenesis by TAA-induction. Notably, the degree of deposition of collagen was deceased in VP-treated group (TAA + VP), compared to TAA-treated fish (Fig. 4Cg–l). Quantitative percentage of collagen proportionate area (CPA) was showed in Fig. 4Ct, which suggested that VP has a potential inhibition effect in TAA-induced fibrosis. Masson's trichrome staining results further validated that TAA-induced zebrafish liver exhibited more collagen fibers compared to control (Fig. 4Cm–r, u). Taken together, these results revealed collagen deposition and fibrosis in TAA-treated zebrafish, whereas no fibrosis was observed TAA + VP and other non-TAA groups.

The next stage, liver fibrosis was assessed through analyzing the expression of markers correlated with collagen deposition, HSCs activation and fibrosis process, including Tgf-β1, Pdgf, α-SMA, Desmin, Vimentin, Smad2 and Snail2. As shown in the expression heat map in Fig. 4Da, in TAA-treatment zebrafish liver, the expression of these molecules was significantly increased, compared with control. The injection of VP and CYC into normal adult fish respectively did not cause significant changes in the factors, while the injection

of VP into TAA-treated zebrafish (TAA + VP) showed that VP significantly inhibited Tgf-β1, Pdgf, Desmin, Vimentin, Smad2 and Snail1. No significant changes were detected in α-SMA expression. CYC also significantly alleviated the increased expression of Desmin, Vimentin and Smad2 in TAA + CYC group, while the inhibition effect of CYC in histology was not detected. All of the results were validated by conventional PCR (Fig. 4Db).

YAP and TAZ proteins are transcriptional coactivators and downstream effectors of the Hippo pathway. When Yap/Taz is activated in cell, dephosphorylated Yap will be translocated into the nucleus further active the downstream Ankrd1, Ctgf and Areg, etc. Here, the expression of Yap target factors was also assessed to evaluated the effect of Yap inhibition in TAA-induced liver injury. It was showed that after induction of TAA, the expression of Yap, Taz and its downstream factors were significantly upregulated. VP injection remarkably inhibited the expression of Yap, Taz and the downstream factors Ankrd1, Ctgf and Areg, which confirmed the targeted inhibitory effect of VP (Fig. 4Dc). In the experimental group of TAA + VP, the expression of Yap, Taz and the downstream set of factors also decreased, compared with individual TAA administration group, with consistence with histology results. Interestingly, CYC also presented suppression activity on expression of Yap and the associated gene set. PCR validation was shown in Fig. 4Dd. Generally, these results implied that Yap knockdown has an inhibitory effect on TAA-induced liver changes in adult zebrafish, which might be related to the Hh signaling involvement.

## Yap and Hh signaling pathway play synergistic protective roles in TAA-induced liver fibrosis

To further validate the correlation of Yap and Hh signaling pathway in TAA-induced liver fibrosis, immunohistochemistry assays were carried on with the detection of α-SMA, YAP and Hh signaling factor GLI2α. Among, α-SMA correlates with activation of fibroblast to myofibroblast, and is an epithelial marker for fibrogenesis (Hinz et al. 2001). The qualitative and quantitative data showed that high expression of α-SMA was found in TAA-treated liver tissue. YAP and GLI2α were also significantly upregulated compared to control ($p < 0.05$). The administration of VP obviously decreased the YAP expression in both VP and TAA + VP groups. VP also played an inhibition role in α-SMA and GLI2α expression. Curiously, compared with TAA-induced fibrotic group, CYC did not show suppression effect on α-SMA expression. However, it decreased the YAP and GLI2α expression in TAA-induction groups, which is consistent with histology and gene expression detection (Fig. 5A, a–d).
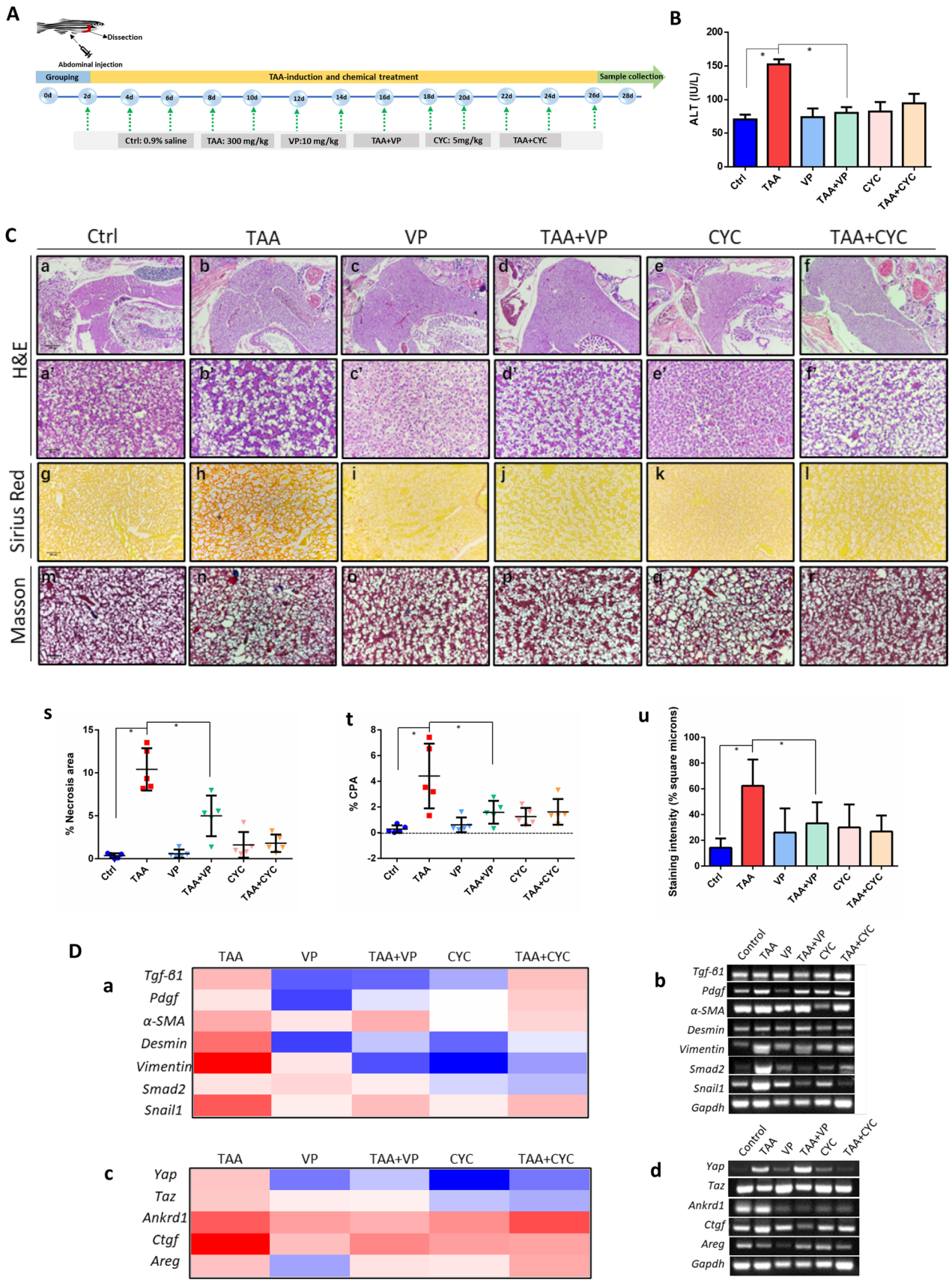
◄**Fig. 4** Assessment of liver histopathology. **A** The experimental flow chart for chemical treatment and time points of sampling. **B** Liver function tests by ALT assay. Statistical test used was one-tailed student t-test, \*$p < 0.05$. **C** Histological evaluations in groups of control, TAA, VP, TAA+VP, CYC and TAA+CYC by hematoxylin and eosin (H&E) staining, collagen secretion (Masson's trichrome staining) and Sirius-red staining in adult zebrafish liver (original magnification 40× and 400×). (**a**) Quantitative measurement of necrotic area in livers; (**b**) Quantitation of Sirius-red staining sections by digital image analysis. (**c**) Quantification of Masson's trichrome staining sections using ImageJ software. Data are reported as collagen proportionate area (CPA) converted into percentage. Five sections of livers per subgroup were analyzed. **D** Quantitative PCR for mRNA expression of liver fibrotic genes (**a**), Yap associated genes (**c**) after TAA treatment in adult zebrafish liver. Conventional PCR was as the validation (**b**, **d**). Values are expressed as means ± SD. \*$p < 0.05$ for treatment groups vs. control

In the embryonic experiment, TAA treatment exhibited a reversal effect on the increase of Hh signal factor Gli1 and Smo, but no obvious effect on Shh (Fig. 3C). In the adult fish treatment experiments, more Hh factors were detected (Fig. 5B). It was found that the expression of Shh, Gli1, Gli2 and Smo were significantly upregulated after TAA treatment. VP inhibited the expression of these four molecules after TAA induction with significance. The expression of other selected two Hh signaling factors, surface receptor ptched (Ptch1) and hedgehog-interacting protein (Hhip) did not show remarkable relevance with neither TAA induction nor Yap inhibitor treatment. In addition, CYC has an inhibitory effect on the expression of Shh and Smo. VP played an inhibition role in TAA-induced Shh, Gli1 and Gli2, which suggested an association of Yap with Hh signaling in the process of liver fibrosis.

## Nuclear colocalization of YAP and GLI2α in TAA-induced liver fibrosis

To further elucidate the potential interaction of Yap and Hh signaling pathway in TAA-induced liver fibrosis, immunofluorescence assays were performed to detect the expression and localization of YAP and Hh signaling factor GLI2α. YAP and GLI2α in liver sections were labeled with red and green fluorescence with corresponding antibodies and nuclei were stained DAPI (blue). Both YAP and GLI2α were constitutively expressed in relatively low expression levels in cells in the absence of TAA (Fig. 6A). However post-TAA induction, expression of YAP and GLI2α were significantly increased compared to control (Fig. 6A, B). YAP was partially translocated into the nucleus and overlapped with GLI2α (Fig. 6A). Quantification of the fluorescent images showed that under TAA-induction, more than 80% of the YAP/GLI2α was colocalized in the nucleus (Fig. 6A, C). All of these observations strongly indicated that TAA induction seems to strengthen the interaction between YAP and GLI2α and promote the nuclear colocalization of YAP and GLI2α.

In summary, a crosstalk exists between Yap and Hh signaling pathway, which may play a synergistic protective role in TAA-induced liver fibrosis (Fig. 7).

## Discussion

Liver fibrosis is traditionally regarded as a progressive pathological process that occurs after extended liver injury with multiple cellular and molecular events, ultimately leading to the excess ECM degradation in the extracellular space (Cai et al. 2020). HSCs are the major source of fibrous matrix-secreting MFs which drive the wound healing fibrogenesis in response to liver injury (Cai et al. 2020). The pathological process is dynamic and theoretically, prevention of the myofibroblastic transdifferentiation of HSCs and limit the excessively accumulation of fibrogenic matrix can reverse the liver fibrogenesis. However, current therapeutic options for liver fibrosis are still limited, and organ transplantation remains the only effective way for end-stage liver cirrhosis. Thus, the mechanisms of orchestrating HSCs activation are attractive therapeutic targets.

Over the past years, several new lines of investigation provide critical insight into molecular mechanism of liver fibrosis and identify important nuclear targets for interfering HSCs activation and reversing liver fibrogenesis. Recent studies suggest Hippo signaling as an important pathway in HSCs activation (Mannaerts et al. 2015). Hippo signaling pathway, originally identified as tissue growth control pathway in Drosophila, has emerged as an integrative component of cellular homeostasis in a variety of tissues (Watt et al. 2017). In mammalian cells, the major kinase cascade is comprised of Mammalian Sterile 20-like kinases 1 and 2 (Mst1/2) and activate the large tumor suppressor kinases 1 and 2 (LATS1/2), which drive phosphorylation and degradation of the transcriptional coactivators, YAP and TAZ (Watt et al. 2017). Upon Hippo pathway inactivation, activated YAP/TAZ translocate into the nucleus and interact with the TEAD family transcription factors, thereby by promoting the expression of target genes of YAP, including Ankrd1, Ctgf, Areg, etc. (Yao et al. 2018). Ankrd1 is a mechano-sensitive transcription factor which mediates TGF-β signaling in response to injury and stress (Kojic et al. 2011). Ctgf is the classic YAP/TAZ target gene which regulates tissue remodeling and repair by regulation of fibronectin, collagens (types I, III, IV, and VI) as well as binding with integrins (Lau 2016). CTGF protein promotes HSCs activation and plays a critical role in a very early stage of fibrotic process (Mannaerts et al. 2015; Friedman 2008), which also implies that YAP drives HSC activation during the initial phase (Mannaerts et al. 2015). AREG is also a down-stream target of YAP which actives epidermal growth factor receptor (EGFR) and plays an important role in ECM environment
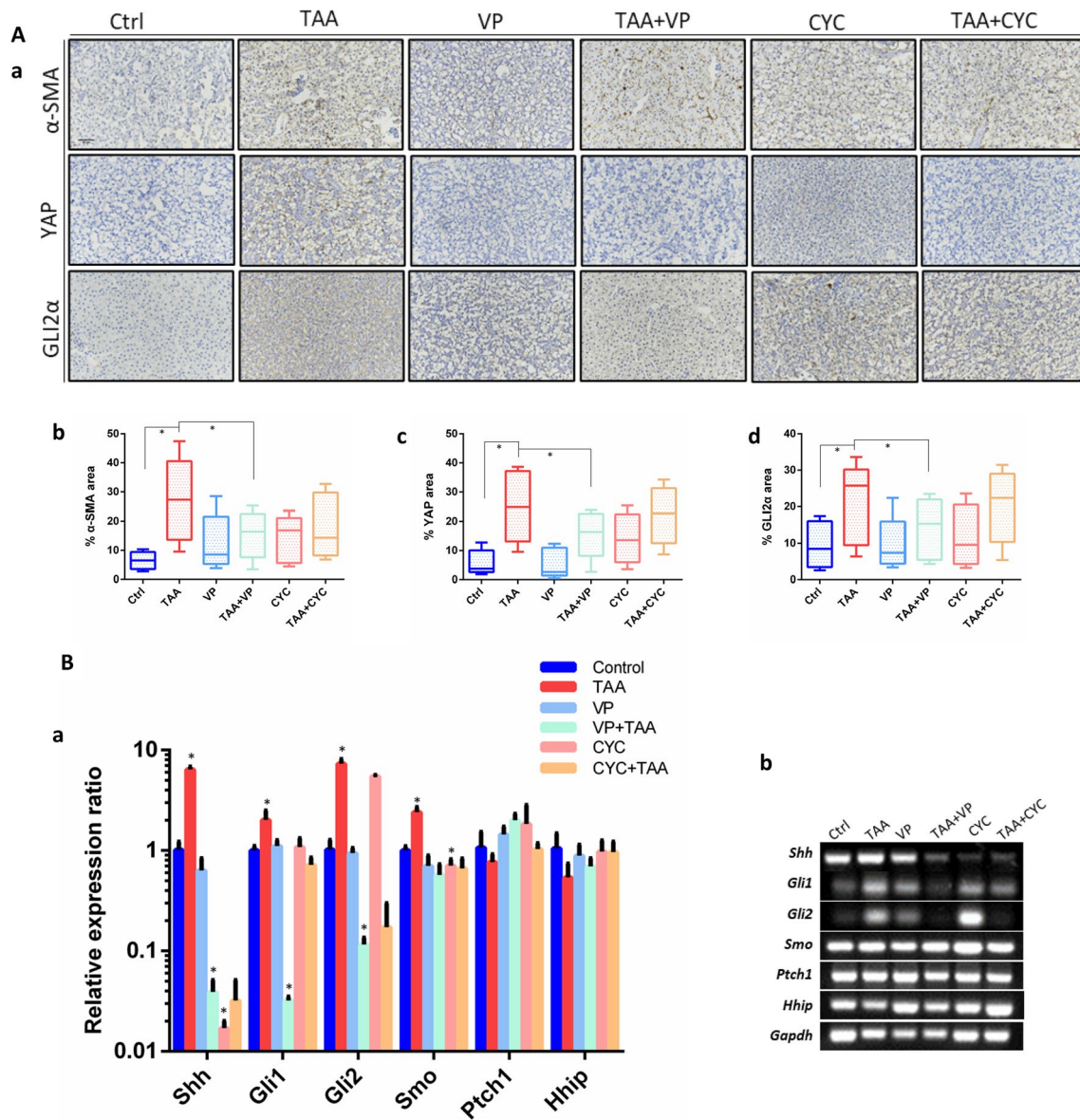
**Fig. 5** Immunohistochemistry detections in zebrafish liver. **A** (**a**) Immunostaining of α-SMA, YAP and GLI2α, for the detection of tissue sections of normal control, TAA-induced, VP treatment, TAA + VP treatment, CYC treatment and TAA + CYC treatment. (**b–d**) Quantitation of α-SMA, YAP and GLI2α immunopositiv-ity by area in the whole liver section in each group. Representative data from 5 slices per group. Scale Bars = 50 μm. **B** Relative expression of Hh factors in adult zebrafish liver. (**a**) QRT-PCR test of factors expression. (**b**) Conventional PCR was as the validation. Data are expressed as the means ± SD. $*p < 0.05$

or blood circulation (Han et al. 2014). In this study, Ankrd1, Ctgf and Areg were chosen to validate the Yap inhibition effect by VP and results were consistent with reported.

It has been reported that YAP activation in HSCs probably provides a molecular basis for hepatocytes fibrosis (Zhubanchaliyev et al. 2016). Sustained YAP activation in liver fibrosis, in part, leads to increased contact between activated HSCs due to pathologic accumulation of ECM proteins and increased focal adhesion formation and tissue stiffness (Dechêne et al. 2010). The mechanical cue of YAP signaling by the influence of matrix stiffness is increasingly

recognized as the main mediator of pathological mechanism (Mannaerts et al. 2015). Importantly, pharmacologic inhibition of YAP by VP that disrupt their respective interactions with cofactors remarkably prevented HSC activation and relieves hepatic fibrogenesis progression of in murine liver fibrosis models (Mannaerts et al. 2015). Thus, Yap represents an attractive potential target prevent HSCs activation and progression of fibrosis. However, the precise function and of YAP in liver fibrosis development was not clearly demonstrated. In this study, the essential roles of Yap in liver fibrosis were investigated by induction of TAA in zebrafish.
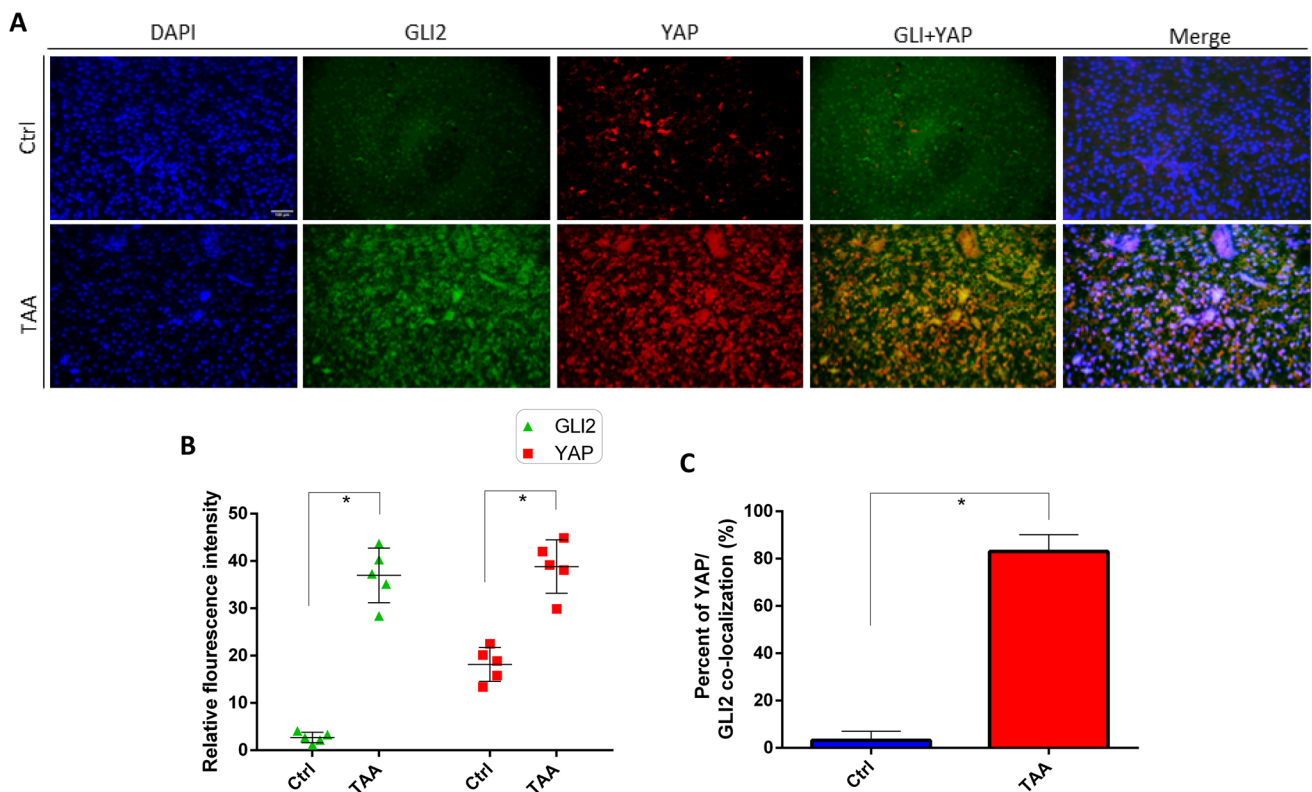
**Fig. 6** Immunohistochemical detection of the distribution of YAP and GLI2α in TAA-induced liver fibrosis. **A** Representative fluorescence microscopy of the distributions of YAP and GLI2α in liver sections using the indicated antibodies: anti-YAP (red), anti-GLI2α (green) and nuclei were stained with 4′, 6-diamidino-2-phenylindole DAPI (blue). The corresponding overlay of YAP and GLI2α is shown in panel (YAP+GLI2α) and the corresponding overlays of the three sig-nals is shown in panel (merge). Scale bar=50 μm. **B** Quantification of relative fluorescence intensity of YAP and GLI2α in control and TAA-induced liver fibrosis. **C** Percent of YAP/GLI2α nuclear colocalization in control and TAA-induced liver fibrosis. The fluorescence intensity of each section was measured by ImageJ. *$p < 0.05$, n=5, means±SD

Yap was detected to be increased in liver fibrosis tissue from a TAA-induced zebrafish model. Embryonic gene knockdown of Yap alleviated TAA-induced embryonic liver lesions. In addition, inhibition of YAP by VP had an inhibitory effect on TAA-induced liver changes in adult zebrafish, which was consist with reported (Mannaerts et al. 2015). These findings supported the potential involvement of YAP in liver fibrosis progression.

The Hippo pathway and its downstream effectors YAP and TAZ, play important roles in various organs in size control, cell differentiation and regeneration in embryonic development and organogenesis (Varelas 2014). While the deletion of Yap results in embryonic lethality or smaller body size with irregular organ development (Varelas 2014). For example knockout of Yap leads to the aberrant retinal pigment epithelium (RPE) specification and development in zebrafish (George et al. 2021). It was reported recently that embryonic knockout of Yap in livers did not show visible defects and disrupted gene function of Yap did not disturb liver bud formation but instead attenuate liver cell proliferation (Yi et al. 2018). Inconsistently, this study demonstrated

that knockdown of Yap expression exhibits the several visible embryonic organ deformities, which is consistent with other reported (Hu et al. 2013). Although Yap is essential for embryogenesis, the loss of yap do not lead to early lethality (Yi et al. 2018). Our findings also highlight this outcome. Nevertheless, in physiological conditions, inhibition of Yap has a certain effect on tissue growth and organ development.

Yap is a morphogenic signaling protein that is relatively inactive in healthy liver. Upon pathological liver injury, the level and activity of YAP change dynamically from homeostasis to overexpressed during the repair process, while deletion of YAP attenuates hepatic fibrosis (Alsamman et al. 2020; Moya and Halder 2019). VP is applied to inhibit YAP through direct binding with its cofactor TAZ, thereby inhibiting the interactions with its downstream cofactors, TEAD1/4 (Liu-Chittenden et al. 2012). Inhibition of Yap by VP leads to the reverse of the chronic HSCs activation and impedes pathological liver fibrosis progression (Mannaerts et al. 2015). For example, ceramide analog, newly discovered as a critical regulator to promote YAP/TAZ degradation and inactivate HSCs, was proved be
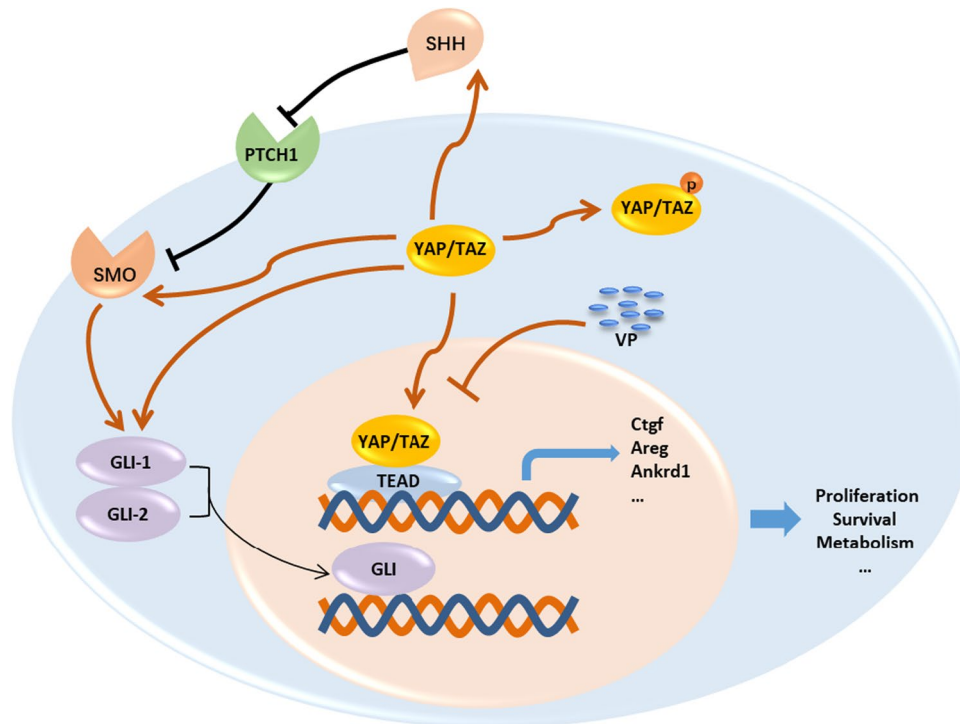
**Fig. 7** Crosstalk between Yap with Hh signaling factors. Upon Hippo pathway inactivation, activated YAP/TAZ translocate into the nucleus and interact with the TEAD family transcription factors, thereby by promoting the expression of target genes of YAP, including Ankrd1, Ctgf, Areg, etc. VP inhibits YAP through direct binding with its cofactor TAZ, thereby inhibiting the interactions with its downstream cofactors, TEAD. Inhibition of Yap exhibited suppression effect on TAA-induced Shh, Smo, Gli1 and Gli2. *YAP* yes-associated protein, *TAZ* transcriptional coactivator with PDZ-binding motif, *VP* verteporfin, *Smo* smoothened, *SHH* sonic hedgehog, *PTCH1* patched 1, *Gli* GLI family zinc finger, *Ctgf* connective tissue growth factor, *Areg* amphiregulin; connective tissue growth factor, *Ankrd1* ankyrin repeat domain 1

efficient for blocking liver fibrosis (Alsamman et al. 2020). In this study, it has been demonstrated that interference of Yap expression by MO (Yap) alleviated liver injury in zebrafish embryos. Additionally, inhibition of YAP by VP attenuated TAA-induced liver fibrosis in adult zebrafish, which were consist with reported (Mannaerts et al. 2015; Mooring et al. 2020). These facts indicate that impeding Yap expression in the early stages of liver injury is an effective prevention of the further deterioration of liver function. Ambivalently, there is conflicting data for negative regulation of YAP/TAZ pathway in liver fibrogenesis. For example, the report by Liu et al. elaborated that Yap activation suppressed HSCs activation and stopped fibrogenesis, while inhibition of YAP by VP exacerbated liver fibrogenesis. Recently Xu et al. also demonstrated that genetic deletion of Yap/Taz in periostin-marked myofibroblasts had no effect on liver fibrogenesis in vivo (Xu et al. 2021). Such discrepancy has triggered controversy regarding the function of YAP/TAZ in liver fibrosis. Collectively, targeted therapy of liver injury and fibrogenesis by YAP inhibitor remains to be broadly assessed. Moreover, further studies are required to determine the comprehensive regulation and the molecular mechanism of Yap.

Hh signaling affects various cellular functions including cell proliferation, cell migration and linage commitment (Ghuloum et al. 2022). During the liver wound healing process, Hh is activated and injured MFs can produce Hh factors Shh and Ihh (Indian hedgehog) ligands during fibrogenesis (Machado and Diehl 2018). Dysregulation of excessive Hh signaling in HSCs leads to pathology in the entire liver. For example, liver injury induces accumulation of factors that activate the Hh pathway which promotes transdifferentiation of HSCs into MF (Gao et al. 2019). Inhibition of Hh signaling in HSCs-derived MF can suppress MF accumulation (Shen et al. 2017), but it can also cause progressive liver injury (Machado and Diehl 2018). Hh is stimulated and activated by several factors accumulate in injured livers, including Pdgf, Tgf-β1, etc. (Machado and Diehl 2018) Shh and Ihh are classic Hh ligands, which are produced in endoderm epithelial cells and secreted to adjacent mesenchymal cells, where the Hh ligands recognize and bind to their receptor Ptch1, resulting in attenuation of the suppression of Smo, which subsequently activate the transcription factors such as Gli1 and Gli2, and finally control the expression of multiple Hh target-genes transcription (Cotton et al. 2017). In this study, Hh signaling factors Gli1, Gli2, Smo and Shh

showed close correlation with TAA induced liver fibrosis. Inhibition of Hh by CYC presented a suppressing role in Hh signals, however, did not exhibit obvious hepatoprotective effect under the induction of TAA, which might because of the dynamic regulation of Hh correlated with the severity and duration of the liver injury (Machado and Diehl 2018). The uncertain mechanisms of Hh in liver damage and repair process remain controversial and need to be further clarified (Machado and Diehl 2018).

In healthy liver, Shh and Hh activity are barely detectable, as well as Yap (Machado and Diehl 2018). However, in HSCs, the activities of both the Hh pathway and Yap change from typical low levels of activity to high activity during liver injury (Swiderska-Syn et al. 2016; Machado and Diehl 2018). The Hh pathway was recently shown to control the activity of YAP in HSCs, and blocking Hh pathway and YAP activation prevented HSCs transdifferentiating into MF (Du et al. 2018). Furthermore, the cross talking between Shh and Yap signaling are correlated with liver injury and Yap is known to be a downstream effect of the Shh pathway in fibrotic livers (Jin et al. 2021). Liver injury triggers the activation of the Hh pathway and Yap, both of which switch from typical low or absent expression levels to high activities (Liu et al. 2019; Swiderska-Syn et al. 2016). Hh pathway directly modulates Yap activation during liver regeneration after partial hepatectomy (PH) and liver fibrosis (Bruschi et al. 2020; Swiderska-Syn et al. 2016; Panciera et al. 2017). Smo, the Hh signaling-competent co-receptor, drives the activation of Yap in myofibroblastic HSCs (Swiderska-Syn et al. 2016). Interruption of Hh signaling in MFs significantly reduced GLI2 and blocked the YAP nuclear accumulation in primary hepatocytes (Swiderska-Syn et al. 2016; Nguyen-Lefebvre et al. 2021). Otherwise, activated Yap transduces many Hh signaling downstream actions in HSC transdifferentiation (Swiderska-Syn et al. 2016). TAZ directly activates Hh signaling with upregulated pro-fibrinogenic factors including osteopontin, Timp1, and Col1a1 (Machado et al. 2015; Manmadhan and Ehmer 2019). Knockdown of Yap inhibits the induction of Hh associated genes, such as Gli1, that is the proximal mediator of the MF transition (Swiderska-Syn et al. 2016; Nguyen-Lefebvre et al. 2021). Hh pathway has been identified to trigger glutaminolysis by interaction with Yap (Du et al. 2018). Taken together, these facts provide novel evidences that HSC fate is mediated by an important cross-talk between YAP and Hh signaling pathway. Our research demonstrated that inhibition of Yap by VP reduced the expression of Shh, Gli1 and Gli2 under induction of TAA. Moreover, disruption of Hh signaling pathway by CYC suppressed the activation of Yap in liver fibrosis. Interestingly, we demonstrate for the first time that the nuclear colocalization of YAP and GLI2α was promoted in TAA-induced liver fibrosis. As known, Gli2 is a downstream target gene of Yap and Yap was identified to

promote tumor angiogenesis through Gli2 (Xu et al. 2019). Gli2 Knockdown rescues the Yap-overexpression phenotype in cortical progenitors (Lin et al. 2012). YAP activity drives GLI2 nuclear accumulation and the nuclear activity of GLI2 and YAP concomitant with increased stromal fibrosis in basal cell carcinoma (Akladios et al. 2017). A complete understanding of the regulation under the nuclear colocalization of YAP and GLI2α and its function in liver fibrosis still require further study.

In this work, to dissect the molecular regulation mechanisms during the initiation of hepatic fibrosis process, the model of TAA-induced liver injury in embryonic and adult zebrafish were utilized following the administration routes and time points as reported (Chuang et al. 2016; Turola et al. 2015; Migdał et al. 2021; Amali et al. 2006b; Katoch and Patial 2021). In summary, this study demonstrates that cross talking of Yap and Hh plays a critical role in liver fibrotic response and provides new theoretical insight concerning the mechanisms of fibrosis progression.

## Declarations

**Conflict of interests** The authors declare no competing interests.

**Ethical approval** This study was approved by the ethics committee of Nanjing Tech University.

**Informed consent** Not applicable.

## References

Akladios B, Mendoza Reinoso V, Cain JE, Wang T, Lambie DL, Watkins DN, Beverdam A (2017) Positive regulatory interactions between YAP and Hedgehog signalling in skin homeostasis and BCC development in mouse skin in vivo. PLoS ONE 12(8):e0183178

Alsamman S, Christenson SA, Yu A, Ayad NM, Mooring MS, Segal JM, Hu JK-H, Schaub JR, Ho SS, Rao V (2020) Targeting acid ceramidase inhibits YAP/TAZ signaling to reduce fibrosis in mice. Sci Transl Med 12(557):1–14

Amali AA, Rekha RD, Lin CJ-F, Wang W-L, Gong H-Y, Her G-M, Wu J-L (2006a) Thioacetamide induced liver damage in zebrafish embryo as a disease model for steatohepatitis. J Biomed Sci 13(2):225–232

Amali AA, Rekha RD, Lin CJ-F, Wang W-L, Gong H-Y, Her G-M, Wu J-L (2006b) Thioacetamide induced liver damage in zebrafish embryo as a disease model for steatohepatitis. J Biomed Sci 13:2

Ballestri S, Nascimbeni F, Romagnoli D, Lonardo A (2016) The independent predictors of non-alcoholic steatohepatitis and its individual histological features. Insulin resistance, serum uric acid, metabolic syndrome, alanine aminotransferase and serum total cholesterol are a clue to pathogenesis and candidate targets for treatment. Hepatol Res 46(11):1074–1087

Brunt EM (2010) Pathology of nonalcoholic fatty liver disease. Nat Rev Gastroenterol Hepatol 7(4):195–203

Bruschi FV, Tardelli M, Einwallner E, Claudel T, Trauner M (2020) PNPLA3 I148M up-regulates hedgehog and yap signaling in human hepatic stellate cells. Int J Mol Sci 21(22):8711

Cai X, Wang J, Wang J, Zhou Q, Yang B, He Q, Weng Q (2020) Intercellular crosstalk of hepatic stellate cells in liver fibrosis: new insights into therapy. Pharmacol Res 155:104720

Choi SS, Omenetti A, Witek RP, Moylan CA, Syn W-K, Jung Y, Yang L, Sudan DL, Sicklick JK, Michelotti GA (2009) Hedgehog pathway activation and epithelial-to-mesenchymal transitions during myofibroblastic transformation of rat hepatic cells in culture and cirrhosis. Am J Physiol Gastrointest Liver Physiol 297(6):G1093–G1106

Chuang H-M, Su H-L, Li C, Lin S-Z, Yen S-Y, Huang M-H, Ho L-I, Chiou T-W, Harn H-J (2016) The role of butylidenephthalide in targeting the microenvironment which contributes to liver fibrosis amelioration. Front Pharmacol. https://doi.org/10.3389/fphar.2016.00112

Cotton JL, Li Q, Ma L, Park J-S, Wang J, Ou J, Zhu LJ, Ip YT, Johnson RL, Mao J (2017) YAP/TAZ and hedgehog coordinate growth and patterning in gastrointestinal mesenchyme. Dev Cell 43(1):35-47.e34

Dechêne A, Sowa JP, Gieseler RK, Jochum C, Bechmann LP, El Fouly A, Schlattjan M, Saner F, Baba HA, Paul A (2010) Acute liver failure is associated with elevated liver stiffness and hepatic stellate cell activation. Hepatology 52(3):1008–1016

Du K, Hyun J, Premont RT, Choi SS, Michelotti GA, Swiderska-Syn M, Dalton GD, Thelen E, Rizi BS, Jung Y (2018) Hedgehog-YAP signaling pathway regulates glutaminolysis to control activation of hepatic stellate cells. Gastroenterology 154(5):1465–1479

Ellis EL, Mann DA (2012) Clinical evidence for the regression of liver fibrosis. J Hepatol 56(5):1171–1180

Fang Y, Liu C, Shu B, Zhai M, Deng C, He C, Luo M, Han T, Zheng W, Zhang J, Liu S (2018) Axis of serotonin-pERK-YAP in liver regeneration. Life Sci 209:490–497

Friedman SL (2008) Hepatic stellate cells: protean, multifunctional, and enigmatic cells of the liver. Physiol Rev 88(1):125–172

Gao H, Bu Y, Wu Q, Wang X, Chang N, Lei L, Chen S, Liu D, Zhu X, Hu K (2015) Mecp2 regulates neural cell differentiation by suppressing the Id1 to Her2 axis in zebrafish. J Cell Sci 128(12):2340–2350

Gao W, Sun J, Wang F, Lu Y, Wen C, Bian Q, Wu H (2019) Deoxyelephantopin suppresses hepatic stellate cells activation associated with inhibition of aerobic glycolysis via hedgehog pathway. Biochem Biophys Res Commun 516(4):1222–1228

George SM, Lu F, Rao M, Leach LL, Gross JM (2021) The retinal pigment epithelium: Development, injury responses, and regenerative potential in mammalian and non-mammalian systems. Prog Retin Eye Res 85:100969

Ghuloum FI, Johnson CA, Riobo-Del Galdo NA, Amer MH (2022) From mesenchymal niches to engineered in vitro model systems: exploring and exploiting biomechanical regulation of vertebrate hedgehog signalling. Mater Today Bio 17:100502

Halder G, Johnson RL (2011) Hippo signaling: growth control and beyond. Development (cambridge, England) 138(1):9–22

Hammes TO, Pedroso GL, Hartmann CR, Escobar TDC, Fracasso LB, da Rosa DP, Marroni NP, Porawski M, da Silveira TR (2012) The effect of taurine on hepatic steatosis induced by thioacetamide in zebrafish (*Danio rerio*). Dig Dis Sci 57(3):675–682

Han S, Bai E, Jin G, He C, Guo X, Wang L, Li M, Ying X, Zhu Q (2014) Expression and clinical significance of YAP, TAZ, and AREG in hepatocellular carcinoma. J Immunol Res 2014:1–10

Henderson JM, Polak N, Chen J, Roediger B, Weninger W, Kench JG, McCaughan GW, Zhang HE, Gorrell MD (2018) Multiple liver insults synergize to accelerate experimental hepatocellular carcinoma. Sci Rep 8(1):1–12

Hinz B, Celetta G, Tomasek JJ, Gabbiani G, Chaponnier C (2001) Alpha-smooth muscle actin expression upregulates fibroblast contractile activity. Mol Biol Cell 12(9):2730–2741

Hu J, Sun S, Jiang Q, Sun S, Wang W, Gui Y, Song H (2013) Yes-associated protein (yap) is required for early embryonic development in zebrafish (*Danio rerio*). Int J Biol Sci 9(3):267–278

Huo X, Li H, Li Z, Yan C, Mathavan S, Liu J, Gong Z (2019a) Transcriptomic analyses of oncogenic hepatocytes reveal common and different molecular pathways of hepatocarcinogenesis in different developmental stages and genders in krasG12V transgenic zebrafish. Biochem Biophys Res Commun 510(4):558–564

Huo X, Li H, Li Z, Yan C, Agrawal I, Mathavan S, Liu J, Gong Z (2019b) Transcriptomic profiles of tumor-associated neutrophils reveal prominent roles in enhancing angiogenesis in liver tumorigenesis in zebrafish. Sci Rep 9(1):1–11

Jiang Q, Liu D, Gong Y, Wang Y, Sun S, Gui Y, Song H (2009) yap is required for the development of brain, eyes, and neural crest in zebrafish. Biochem Biophys Res Commun 384(1):114–119

Jin L, Huang H, Ni J, Shen J, Liu Z, Li L, Fu S, Yan J, Hu B (2021) Shh-Yap signaling controls hepatic ductular reactions in CCl$_4$-induced liver injury. Environ Toxicol 36(2):194–203

Johnson RL (2019) Hippo signaling and epithelial cell plasticity in mammalian liver development, homeostasis, injury and disease. Sci China Life Sci 62(12):1609–1616

Katoch S, Patial V (2021) Zebrafish: an emerging model system to study liver diseases and related drug discovery. J Appl Toxicol 41(1):33–51

Kinkel MD, Eames SC, Philipson LH, Prince VE (2010) Intraperitoneal injection into adult zebrafish. JoVE 42:e2126

Kisseleva T, Brenner DA (2008) Mechanisms of fibrogenesis. Exp Biol Med 233(2):109–122

Kojic S, Radojkovic D, Faulkner G (2011) Muscle ankyrin repeat proteins: their role in striated muscle function in health and disease. Crit Rev Clin Lab Sci 48(5–6):269–294

Kumar V, Dong Y, Kumar V, Almawash S, Mahato RI (2019) The use of micelles to deliver potential hedgehog pathway inhibitor for the treatment of liver fibrosis. Theranostics 9(25):7537–7555

Lam SH, Wu YL, Vega VB, Miller LD, Spitsbergen J, Tong Y, Zhan H, Govindarajan KR, Lee S, Mathavan S (2006) Conservation of gene expression signatures between zebrafish and human liver tumors and tumor progression. Nat Biotechnol 24(1):73–75

Lau LF (2016) Cell surface receptors for CCN proteins. J Cell Commun Signal 10(2):121–127

Lee EH, Park KI, Kim KY, Lee JH, Jang EJ, Ku SK, Kim SC, Suk HY, Park JY, Baek SY, Kim YW (2019) Liquiritigenin inhibits hepatic fibrogenesis and TGF-β1/Smad with Hippo/YAP signal. Phytomedicine 62:152780

Li R, Cai L, Ding J, Hu CM, Wu TN, Hu XY (2015) Inhibition of hedgehog signal pathway by cyclopamine attenuates inflammation and articular cartilage damage in rats with adjuvant-induced arthritis. J Pharm Pharmacol 67(7):963–971

Lin Y-T, Ding J-Y, Li M-Y, Yeh T-S, Wang T-W, Yu J-Y (2012) YAP regulates neuronal differentiation through Sonic hedgehog signaling pathway. Exp Cell Res 318(15):1877–1888

Lin H, Huang Y, Tian T, Wang P, Li Y (2020) Propionate promotes vitamin D receptor expression via yes-associated protein in rats with short bowel syndrome. Biochem Biophys Res Commun 523(3):645–650

Liu Y, Lu T, Zhang C, Xu J, Xue Z, Busuttil RW, Xu N, Xia Q, Kupiec-Weglinski JW, Ji H (2019) Activation of YAP attenuates hepatic damage and fibrosis in liver ischemia-reperfusion injury. J Hepatol 71(4):719–730

Liu-Chittenden Y, Huang B, Shim JS, Chen Q, Lee S-J, Anders RA, Liu JO, Pan D (2012) Genetic and pharmacological disruption of the TEAD–YAP complex suppresses the oncogenic activity of YAP. Genes Dev 26(12):1300–1305

Livak KJ, Schmittgen TD (2001) Analysis of relative gene expression data using real-time quantitative PCR and the $2^{-\Delta\Delta CT}$ method. Methods 25(4):402–408

Lodyga M, Hinz B (2020) TGF-β1–a truly transforming growth factor in fibrosis and immunity. In: Proceedings of the seminars in cell and developmental biology. Elsevier, pp 123–139

Ma H-Y, Yamamoto G, Xu J, Liu X, Karin D, Kim JY, Alexandrov LB, Koyama Y, Nishio T, Benner C (2020) IL-17 signaling in steatotic hepatocytes and macrophages promotes hepatocellular carcinoma in alcohol-related liver disease. J Hepatol 72(5):946–959

Machado MV, Diehl AM (2018) Hedgehog signalling in liver pathophysiology. J Hepatol 68(3):550–562

Machado MV, Michelotti GA, Pereira TA, Xie G, Premont R, Cortez-Pinto H, Diehl AM (2015) Accumulation of duct cells with activated YAP parallels fibrosis progression in non-alcoholic fatty liver disease. J Hepatol 63(4):962–970

Manmadhan S, Ehmer U (2019) Hippo signaling in the liver–a long and ever-expanding story. Front Cell Dev Biol 7:33

Mannaerts I, Leite SB, Verhulst S, Claerhout S, Eysackers N, Thoen LF, Hoorens A, Reynaert H, Halder G, van Grunsven LA (2015) The Hippo pathway effector YAP controls mouse hepatic stellate cell activation. J Hepatol 63(3):679–688

Migdał M, Tralle E, Nahia KA, Bugajski Ł, Kędzierska KZ, Garbicz F, Piwocka K, Winata CL, Pawlak M (2021) Multi-omics analyses of early liver injury reveals cell-type-specific transcriptional and epigenomic shift. BMC Genom 22:1–15

Mooring M, Fowl BH, Lum SZ, Liu Y, Yao K, Softic S, Kirchner R, Bernstein A, Singhi AD, Jay DG (2020) Hepatocyte stress increases expression of yes-associated protein and transcriptional coactivator with PDZ-binding motif in hepatocytes to promote parenchymal inflammation and fibrosis. Hepatology 71(5):1813–1830

Moya IM, Halder G (2019) Hippo–YAP/TAZ signalling in organ regeneration and regenerative medicine. Nat Rev Mol Cell Biol 20(4):211–226

Nguyen Q, Anders RA, Alpini G, Bai H (2015) Yes-associated protein in the liver: regulation of hepatic development, repair, cell fate determination and tumorigenesis. Dig Liver Dis 47(10):826–835

Nguyen-Lefebvre AT, Selzner N, Wrana JL, Bhat M (2021) The hippo pathway: a master regulator of liver metabolism, regeneration, and disease. FASEB J 35(5):e21570

Oh SH, Swiderska-Syn M, Jewell ML, Premont RT, Diehl AM (2018) Liver regeneration requires Yap1-TGFβ-dependent epithelial-mesenchymal transition in hepatocytes. J Hepatol 69(2):359–367

Panciera T, Azzolin L, Cordenonsi M, Piccolo S (2017) Mechanobiology of YAP and TAZ in physiology and disease. Nat Rev Mol Cell Biol 18(12):758–770

Reimer MM, Kuscha V, Wyatt C, Sörensen I, Frank RE, Knüwer M, Becker T, Becker CG (2009) Sonic hedgehog is a polarized signal for motor neuron regeneration in adult zebrafish. J Neurosci 29(48):15073–15082

Rekha RD, Amali AA, Her GM, Yeh YH, Gong HY, Hu SY, Lin GH, Wu JL (2008) Thioacetamide accelerates steatohepatitis, cirrhosis

and HCC by expressing HCV core protein in transgenic zebrafish *Danio rerio*. Toxicology 243(1–2):11–22

Rockey DC, Bell PD, Hill JA (2015) Fibrosis—a common pathway to organ injury and failure. N Engl J Med 372(12):1138–1149

Seki E, Schwabe RF (2015) Hepatic inflammation and fibrosis: functional links and key pathways. Hepatology 61(3):1066–1079

Shen X, Peng Y, Li H (2017) The injury-related activation of hedgehog signaling pathway modulates the repair-associated inflammation in liver fibrosis. Front Immunol 8:1450

Subramanian A, Tamayo P, Mootha VK, Mukherjee S, Ebert BL, Gillette MA, Paulovich A, Pomeroy SL, Golub TR, Lander ES (2005) Gene set enrichment analysis: a knowledge-based approach for interpreting genome-wide expression profiles. Proc Natl Acad Sci 102(43):15545–15550

Swiderska-Syn M, Xie G, Michelotti GA, Jewell ML, Premont RT, Syn WK, Diehl AM (2016) Hedgehog regulates yes-associated protein 1 in regenerating mouse liver. Hepatology 64(1):232–244

Turola E, Milosa F, Critelli R, di Giovanni M, Cotelli F, Villa E (2015) Overfeeding accelerates thioacetamide-induced liver damage in zebrafish

van der Helm D, Groenewoud A, de Jonge-Muller ES, Barnhoorn MC, Schoonderwoerd MJ, Coenraad MJ, Hawinkels LJ, Snaar-Jagalska BE, van Hoek B, Verspaget HW (2018) Mesenchymal stromal cells prevent progression of liver fibrosis in a novel zebrafish embryo model. Sci Rep 8(1):1–11

Varelas X (2014) The Hippo pathway effectors TAZ and YAP in development, homeostasis and disease. Development (cambridge, England) 141(8):1614–1626

Villesen IF, Daniels SJ, Leeming DJ, Karsdal MA, Nielsen MJ (2020) the signalling and functional role of the extracellular matrix in the development of liver fibrosis. Aliment Pharmacol Ther 52(1):85–97

Wang Y, Chen W, Han C, Zhang J, Song K, Kwon H, Dash S, Yao L, Wu T (2018) Adult hepatocytes are hedgehog-responsive cells in the setting of liver injury: evidence for smoothened-mediated activation of NF-κB/epidermal growth factor receptor/Akt in hepatocytes that counteract Fas-induced apoptosis. Am J Pathol 188(11):2605–2616

Watt KI, Harvey KF, Gregorevic P (2017) Regulation of tissue growth by the mammalian hippo signaling pathway. Front Physiol 8:942

Wells RG, Schwabe RF (2015) Origin and function of myofibroblasts in the liver. In: Proceedings of the seminars in liver disease. Thieme Medical Publishers, pp 097–106

Xu S, Zhang H, Chong Y, Guan B, Guo P (2019) YAP promotes VEGFA expression and tumor angiogenesis though Gli2 in human renal cell carcinoma. Arch Med Res 50(4):225–233

Xu L, Wettschureck N, Bai Y, Yuan Z, Wang S (2021) Myofibroblast YAP/TAZ is dispensable for liver fibrosis in mice. J Hepatol 75:238–241

Yan J, Huang H, Liu Z, Shen J, Ni J, Han J, Wang R, Lin D, Hu B, Jin L (2020) Hedgehog signaling pathway regulates hexavalent chromium-induced liver fibrosis by activation of hepatic stellate cells. Toxicol Lett 320:1–8

Yao F, Zhou Z, Kim J, Hang Q, Xiao Z, Ton BN, Chang L, Liu N, Zeng L, Wang W (2018) SKP2-and OTUD1-regulated non-proteolytic ubiquitination of YAP promotes YAP nuclear localization and activity. Nat Commun 9(1):1–16

Yi X, Yu J, Ma C, Li L, Luo L, Li H, Ruan H, Huang H (2018) Yap1/Taz are essential for the liver development in zebrafish. Biochem Biophys Res Commun 503(1):131–137

Yu H, Yao Y, Bu F, Chen Y, Wu Y, Yang Y, Chen X, Zhu Y, Wang Q, Pan X (2019) Blockade of YAP alleviates hepatic fibrosis through accelerating apoptosis and reversion of activated hepatic stellate cells. Mol Immunol 107:29–40

Yu D, Liu H, Qin J, Huangfu M, Guan X, Li X, Zhou L, Dou T, Liu Y, Wang L, Fu M, Wang J, Chen X (2021) Curcumol inhibits the

viability and invasion of colorectal cancer cells via miR-30a-5p and Hippo signaling pathway. Oncol Lett 21(4):299

Zhang Y, Zhang X, Cui L, Chen R, Zhang C, Li Y, He T, Zhu X, Shen Z, Dong L, Zhao J, Wen Y, Zheng X, Li P (2017) Salvianolic acids for injection (SAFI) promotes functional recovery and neurogenesis via sonic hedgehog pathway after stroke in mice. Neurochem Int 110:38–48

Zhao Y, Huang X, Ding TW, Gong Z (2016) Enhanced angiogenesis, hypoxia and neutrophil recruitment during Myc-induced liver tumorigenesis in zebrafish. Sci Rep 6(1):1–12

Zhao Y, Wang H-L, Li T-T, Yang F, Tzeng C-M (2020) Baicalin ameliorates dexamethasone-induced osteoporosis by regulation of the RANK/RANKL/OPG signaling pathway. Drug Des Dev Ther 14:195

Zhubanchaliyev A, Temirbekuly A, Kongrtay K, Wanshura LC, Kunz J (2016) Targeting mechanotransduction at the transcriptional level: YAP and BRD4 are novel therapeutic targets for the reversal of liver fibrosis. Front Pharmacol. https://doi.org/10.3389/fphar.2016.00462